Mathematical Biosciences and Engineering

https://www.aimspress.com/journal/mbe

MBE, 23(6): 1708–1742.
DOI: 10.3934/mbe.2026062
Received: 23 September 2025
Revised: 12 November 2025
Accepted: 25 November 2025
Published: 19 May 2025

Research article

Fractional gender structured model of human papillomavirus (HPV)

Veysel Fuat Hatipoğlu1[1,*] **and Maia Martcheva**[2]

[1] Department of Business Administration, Fethiye Faculty of Management, Muğla Sıtkı Koçman University, Muğla 48300, Turkey

[2] Department of Mathematics, University of Florida, Gainesville, FL 32611, USA

* **Correspondence:** Email: veyselfuat.hatipoglu@mu.edu.tr.

Abstract: We propose a fractional-order differential equation model to study the gender-specific transmission dynamics of human papillomavirus (HPV). Due to limited gender-disaggregated HPV data, oropharyngeal cancer incidence was used as a proxy. The model includes a theoretical analysis of disease-free and endemic equilibria and computation of the basic reproduction number, with stability conditions derived for both cases. Structural identifiability was confirmed using differential algebra, and data fitting indicated that the fractional models ($\alpha = 0.9$) better captured U.S. dynamics, while classical models ($\alpha = 1$) suited Turkish data. Practical identifiability, assessed via Monte Carlo simulations, revealed that most parameters were identifiable, though some (e.g., the male exit rate μ_m) showed limitations. Numerical simulations demonstrated sensitivity to fractional effects. This work provides a robust framework for modeling the transmission of HPV and offers insights for future epidemiological modeling and intervention planning.

Keywords: HPV; two-sex model; fractional order epidemiological model; structural identifiability; practical identifiability; parameter estimation

1. Introduction

Human papillomavirus (HPV) is a class of 200 viruses that spread through sexual contact [1]. Human papillomaviruses are divided into two groups: high risk and low risk. High-risk viruses, particularly HPV 16 and HPV 18, cause most cancers that result from HPV infection. Low-risk viruses rarely lead to cancer. While most HPV infections are asymptomatic and resolve themselves within a couple of years [2], it is that connection to cancer that makes HPV important to study. HPV's prevalence in Turkey is between 2% and 46% in some regions [3], while in the US, HPV's prevalence is estimated at around 40% [4]. In Turkey, about 4.2% of the women in the general population harbor HPV 16/18 [5, 6], and in the US about 3.9% of all women at any time are infected with genotypes

HPV 16/18 [7].

Mathematical modeling of HPV is a powerful tool that can help stakeholders to compare different prevention and mitigation measures for the control of HPV and HPV-related cancers. Mathematical models of HPV and the resulting cancers are predominantly ordinary differential equation (ODE) models. Early modeling focused on HPV and cervical cancer as the most prevalent cancer resulting from HPV infection in women. Lee and Tameru developed a single-gender model that incorporates HPV infection and cervical cancer in US African-American women [8]. Sado [9] considered an ODE model of cervical cancer and HPV transmission and vaccination. Zhang et al. [10] considered a somewhat more elaborate model of HPV infection with cervical cancer. Dasbach et al. [11] investigated several types of models that discuss the role of HPV infection on cervical cancer. Imperfect vaccination leads to backward bifurcation in a model of HPV transmission that leads to cancer [12]. The impact of vaccination on HPV infections and cervical cancer was recently investigated in [13]. Liu et al. [14] considered the relation of HPV infection and cervical cancer in Hungary. The models in these articles are all ODE and single-gender models.

Two-sex models of HPV have also been considered. Elbasha [15] developed one of the first HPV two-sex models. Other two-sex models of HPV also followed but in many cases, they did not include cancers. Omame et al. considered a two-sex model with imperfect vaccine and prevention strategies [16]. Sharomi et al. included HPV and cervical cancer in a two-sex model [17]. In a series of papers, Gao et al. considered two-sex models of HPV without the inclusion of cancer [18–20]. Saldana et al. [21] considered a female-male model of HPV and its relation to HPV-induced female and male cancers. All these models were ODE models. Al-arydah and Smith considered an age-structured partial differential equation (PDE) two-sex model of HPV infection with vaccination [22].

Fractional differential equations (FDEs) involve time derivatives of fractional order and are used to model memory in a system. FDEs are becoming increasingly popular as models in biology in general and epidemiology in particular. The Caputo fractional derivative is used in biological modeling to represent processes that have a memory or history-dependent behavior, meaning that the system's current state depends on its past states, not just its immediate past. Unlike classical integer-order derivatives, which only consider the instantaneous rate of change, the Caputo fractional derivative is a "non local" operator that incorporates information from the function's entire history over a given time interval [23, 24]. Recently, Chen et al. [25] reviewed fractional epidemic models, giving us a glimpse of the importance and applicability of FDEs in modeling infectious disease transmission. HPV infection and transmission have been studied with fractional-order differential equation models. Zafar et al. [26] introduced and studied on FDE model of HPV with the Atangana-Baleanu fractional derivative. Nwajeri et al. studied a coinfection model of HPV and *Chlamydia trachomatis* using the Caputo fractional derivative [27]. El-Mesady et al. [28] implemented a fractional-order optimal control problem to investigate the outcomes of HPV infection. Bahi et al. [29] used the Caputo derivative to model HPV and cervical cancer, giving recommendations to public health officials. Bajjah [30] et al. developed a finite difference method for a HPV model with the Caputo fractional derivative. Raza et al. [31] introduced an FDE of HPV transmission with the Atangana-Baleanu fractional derivative and studied the association of HPV with cervical cancer. In a sequence of articles, Rajan et al. [32, 33] introduced an HPV model with the Caputo fractional derivative and then used it to study cervical cancer. Hattaf [34] introduced a new fractional derivative definition for some

applications in computational biology which encompasses many types of fractional derivatives such as the Caputo fractional derivative and the Atangana-Baleanu fractional derivative. In some articles [35, 36], the authors used the Hattaf fractional derivative for FDEs arising in models of pharmacokinetics and virus dynamics.

The Caputo derivative is used in this paper because it provides a relatively more accurate representation of biological processes compared with standard integer-order models, as it allows for the incorporation of memory effects and initial conditions, which are crucial in biological systems. The Caputo derivative is better suited for biological modeling, as it can capture how a system's past states influence its present behavior, which is essential for modeling complex phenomena like the spread of HPV. Biological processes are often characterized by long-term dependencies and complex interactions, which are, in some cases (as we show), more accurately captured by fractional-order derivatives like the Caputo derivative [37].

While fractional derivative models have played significant role both in epidemic modeling in general and in HPV and cervical cancers in particular, there seems to be little work done in connecting these models to data and in studying the identifiability of these models. Few of the FDE models of HPV and cancer have been linked to data, and, consequently, the structural and practical identifiability of these models have not been studied (but see [38]). The work of Kharazmi et al. [38] is pioneering in the identifiability of fractional-order epidemiological models. However, their results are mainly simulations and do not address the structural identifiability analytically. Our article contributes in several ways to the FDE HPV modeling literature. First, we consider a two-sex FDE model with the Caputo derivative. Second, given data on male and female cancer incidence, we examine the structural identifiability of the model using the differential algebra approach. Third, we use male and female data on oropharyngeal cancer in the US and Turkey to fit the model and perform a practical identifiability analysis of the parameters. The motivation for this study is to understand the spread of HPV in Turkey and its impact on cancer, and to compare Turkey's results with those in the US, so that Turkey's HPV distribution can be viewed in more global context.

This paper is structured as follows. In the next section, we introduce the FDE HPV model. In Section 3, we compute the reproduction number and perform an analysis of the model. In Section 4, we examine the structural identifiability of the model relative to male and female cancer data. In Section 5, we fit the model to the data, and test its practical identifiability. In Section 6, we perform some simulations with varying parameters. Section 7 summarizes our results.

2. Model formulation

This section introduces a deterministic two-sex fractional-order model designed to analyze the spread of HPV in a sexually active population. The model classifies individuals into four compartments which consist of two compartments, namely susceptible and infected for each gender. The recruitment rate for new susceptible individuals who become sexually active and enter the susceptible compartment S_k is denoted by Λ_k, where $k = f, m$. Individuals leave a compartment at a rate μ_k. Susceptible individuals are infected by HPV with a force of infection λ_k. Those infected move to the infected compartment I_k. Infected individuals can clear the infection at a rate δ_k. While natural recovery can offer protection against future infection for many other viral infections, several studies show that reinfection can occur after recovery from HPV [39–41].

2.1. The fractional-order model

The model assumes a population divided into two gender groups, where individuals transition between susceptible and infected states. The rate of infection depends on contact patterns between the genders and the probability of transmission. In the model, we modify the system constructed in [20] by replacing the standard time derivative with the Caputo fractional derivative [42], denoted by $\mathbf{D}^{\alpha}$, where α is the fractional order $0 < \alpha < 1$ of the derivative. In mathematical biology, the analysis revolves around equilibria or time-independent solutions. This requires the derivative of a constant to be zero, which is a property of the Caputo derivative. Moreover, the Caputo derivative handles well with initial value problems and it is close to ODEs' integer orders, which are the main reasons for the choice of the Caputo derivative for the memory effect of the system. In some studies [43, 44], the authors showed that fractional-order derivatives with the Caputo derivative fit better to biological models. However, the fractional-order derivative adjustment causes the dimensions of the two sides of the equation to become unequal. To address this, we introduce an auxiliary parameter representing the fractional time components in the system [45], where γ is a parameter that encompasses the fractional dimension of the memory effect in the Caputo derivative, which has the unit of $1/time$ (see the Appendix), in order to scale the fractional operator and ensure that the dimensions are consistent on both sides. As explained, the fractional model for the transmission of the human papilloma virus for $t > 0$ and $\alpha \in (0, 1)$ is represented by

$$\begin{aligned}
\gamma^{\alpha-1}\mathbf{D}_t^{\alpha} S_f(t) &= \Lambda_f - \lambda_f S_f + \delta_f I_f - \mu_f S_f, && (2.1)\\
\gamma^{\alpha-1}\mathbf{D}_t^{\alpha} I_f(t) &= \lambda_f S_f - \delta_f I_f - \mu_f I_f, && (2.2)\\
\gamma^{\alpha-1}\mathbf{D}_t^{\alpha} S_m(t) &= \Lambda_m - \lambda_m S_m + \delta_m I_m - \mu_m S_m, && (2.3)\\
\gamma^{\alpha-1}\mathbf{D}_t^{\alpha} I_m(t) &= \lambda_f S_m - \delta_m I_m - \mu_m I_m && (2.4)
\end{aligned}$$

with the infection force $\lambda_f = \frac{\beta_{mf} I_m}{N_f}$ and $\lambda_m = \frac{\beta_{fm} I_f}{N_m}$, where S_k and I_k represent the susceptible and infected populations, respectively, for gender k, and $N_k = S_k + I_k$. Summation of (2.1)–(2.4) results in $\mathbf{D}_t^{\alpha} N_k(t) = \gamma^{1-\alpha}(\Lambda_k - \mu_k N_k)$. $\mathbf{D}_t^{\alpha} N_k(t) = 0$, so we have $\gamma^{1-\alpha}(\Lambda_k - \mu_k N_k) = 0$. Since $\gamma \neq 0$, we have $\Lambda_k - \mu_k N_k = 0$ and then $N_k = \Lambda_k/\mu_k$. Therefore, the equilibria of N_f and N_m are Λ_f/μ_f and Λ_m/μ_m, respectively. We also have a total population size $N = N_f + N_m$. Domain D of the system (2.1)–(2.4) is defined as

$$D = \left\{(S_f, I_f, S_m, I_m) \in R_+^4 : S_k + I_k \leq \Lambda_k/\mu_k, k = f, m\right\}. \quad (2.5)$$

The flowchart of the system (2.1)–(2.4) is presented in Figure 1.

A description of the variables, parameters, and subscripts given in the systems (2.1)–(2.4) are provided in Tables 1, 2, and 3.

Table 1. Description of the subscripts of the parameters.

Symbol	Description
Subscripts	
f	Female
m	Male
k	Gender ($k = f, m$)

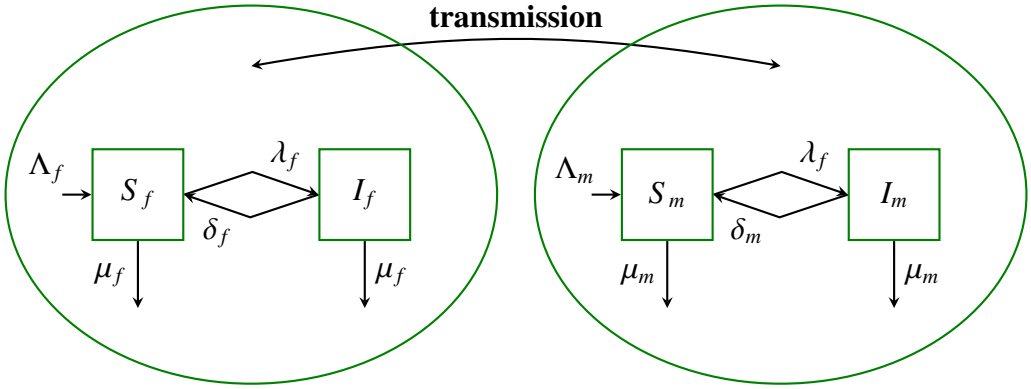

Figure 1. Flow diagram of the models (2.1)–(2.4).

Table 2. Description of the variables.

Symbol	Description
Variables	
$S_k(t)$	Susceptible population of gender k
$I_k(t)$	Infected population of gender k
$N_k(t)$	Total size of the population of gender k
$N(t)$	Total size of the population
λ_k	Force of infection for gender k

Table 3. Description of the parameters.

Symbol	Description	Unit
Parameters		
β_{fm}	Transmission rate (females to males)	1/year
β_{mf}	Transmission rate (males to females)	1/year
δ_f	Recovery rate (female)	1/year
δ_m	Recovery rate (male)	1/year
Λ_f	Recruitment into sexually active females	person/year
Λ_m	Recruitment into sexually active males	person/year
μ_f	Exit rate from sexually active females	1/year
μ_m	Exit rate from sexually active males	1/year
γ	Auxilary parameter	1/year

In order to show the well-posedness of the models (2.1)–(2.4) both mathematically and epidemiologically, it is possible to verify, by using similar method as in [18], that the domain D is positively invariant for the systems (2.1)–(2.4).

3. Mathematical analysis of the model

3.1. Disease-free equilibrium and basic reproduction number

The reproduction number R_0 signifies the total count of infections spread by a single infected person across an entirely vulnerable population over the duration of their infectious phase. It is derived using the next-generation approach [46], providing insights into disease persistence as follows:

$$R_0 = \sqrt{R_{0,mf}R_{0,fm}}, \tag{3.1}$$

where:

$$R_{0,mf} = \frac{\beta_{mf}}{\delta_f + \mu_f}, \tag{3.2}$$

$$R_{0,fm} = \frac{\beta_{fm}}{\delta_m + \mu_m}. \tag{3.3}$$

The term $R_{0;mf}$ indicates the total count of secondary infections in females caused by a single infected male throughout his entire period of infection, assuming that all females in the population are susceptible. Similarly, the term $R_{0;fm}$ conveys a comparable concept. The disease-free equilibrium of the systems (2.1)–(2.4) is $E^0 = (\Lambda_f/\mu_f, 0, \Lambda_m/\mu_m, 0)$.

3.2. Stability analysis of equilibria

The system is analyzed for local and global stability under different conditions. Using the linearization technique, the stability of both disease-free and endemic equilibria is determined. Theorem 2 presents the stability conditions of the disease-free equilibrium E^0. First, we present the following result introduced in [47, 48] to prove the stability of the system.

Theorem 1. *The autonomous fractional-order system*

$$\mathbf{D}^{\alpha}\mathbf{x}(t) = A\mathbf{x}(t), \mathbf{x}(0) = \mathbf{x}_0, \tag{3.4}$$

where $\mathbf{x} \in \mathbb{R}^n$*, the matrix* $A \in \mathbb{R}^n \times \mathbb{R}^n$*, and* $0 < \alpha \leq 1$ *indicates the fractional orders defined as the Caputo fractional derivative, is asymptotically stable if and only if* $|\arg(spec(A))| > \frac{\alpha\pi}{2}$.

Theorem 2. *When* $R_0 < 1$*, the disease-free equilibrium* E^0 *is locally asymptotically stable. When* $R_0 > 1$*, it becomes unstable.*

Proof. The matrix A in the system (3.4) is the same as that for the ODE and FDE systems. Therefore, the spectrum is the same. The study of the ODE system [20] has negative real parts for the eigenvalues. Two of these eigenvalues are $-\mu_f$ and $-\mu_m$, which holds for our matrix A for the systems (2.1)–(2.4), i.e., $-\gamma^{\alpha-1}\mu_f$ and $-\gamma^{\alpha-1}\mu_m$. The other two eigenvalues are $\lambda = \gamma^{\alpha-1}\frac{-(a+b)\pm\sqrt{(a+b)^2-4(ab-\beta_{mf}\beta_{fm})}}{2}$, where $a = \delta_f + \mu_f, b = \delta_m + \mu_m$. If $R_0 < 1$, then the corresponding ODE system of (2.1)–(2.4) has only eigenvalues with negative real parts. Therefore, the FDE systems (2.1)–(2.4) is stable by Theorem 1. If $R_0 > 1$, then there is always a real positive eigenvalue for the corresponding ODE system. This implies that FDE system is also unstable. □

Theorem 3. *The disease-free equilibrium E^0 is globally asymptotically stable, when $R_0 \leq 1$.*

Proof. The dynamişcs of the given model are equivalent to the dynamics of the limiting model, where $N_f(t) \to \frac{\Lambda_f}{\mu_f} = N_f^*$ and $N_m(t) \to \frac{\Lambda_m}{\mu_m} = N_m^*$. We then rewrite the parameters $\bar{\lambda}_f = \frac{\beta_{mf} I_m}{N_f^*}$ and $\bar{\lambda}_m = \frac{\beta_{fm} I_f}{N_m^*}$. Let us consider the Lyapunov function

$$V = \left(S_f - S_f^0 - S_f^0 \ln \frac{S_f}{S_f^0} + I_f \right) + R_{0,mf} \left(S_m - S_m^0 - S_m^0 \ln \frac{S_m}{S_m^0} + I_m \right),$$

where $S_f^0 = N_f^*$ and $S_m^0 = N_m^*$. One can see that V is radially unbounded and positive definite in the entire space. Applying the Caputo fractional derivative on both sides and applying Lemma 3.1 in [49], we have

$$\mathbf{D}_t^\alpha V \leq \left[\left(1 - \frac{S_f^0}{S_f} \right) \mathbf{D}_t^\alpha S_f + \mathbf{D}_t^\alpha I_f \right] + R_{0,mf} \left[\left(1 - \frac{S_m^0}{S_m} \right) \mathbf{D}_t^\alpha S_m + \mathbf{D}_t^\alpha I_m \right].$$

From the systems (2.1)–(2.4) we get

$$\begin{aligned} \mathbf{D}_t^\alpha V \leq & \left[\left(1 - \frac{S_f^0}{S_f} \right) (\Lambda_f - \bar{\lambda}_f S_f + \delta_f I_f - \mu_f S_f) + (\bar{\lambda}_f S_f - (\delta_f - \mu_f) I_f) \right] \gamma^{1-\alpha} \\ & + R_{0,mf} \left[\left(1 - \frac{S_m^0}{S_m} \right) (\Lambda_m - \bar{\lambda}_m S_m + \delta_m I_m - \mu_m S_m) + (\bar{\lambda}_m S_m - (\delta_m - \mu_m) I_m) \right] \gamma^{1-\alpha}. \end{aligned}$$

Using the equilibrium conditions $\Lambda_f = \mu_f S_f^0$, $\Lambda_m = \mu_m S_m^0$, $N_f^* = S_f^0$, $N_m^* = S_m^0$, $\frac{S_f^0}{S_f} \geq 1$, and $\frac{S_m^0}{S_m} \geq 1$ and adding the terms we get

$$\begin{aligned} \mathbf{D}_t^\alpha V \leq & \left[\left(1 - \frac{S_f^0}{S_f} \right) \mu_f (S_f^0 - S_f) + S_f^0 \bar{\lambda}_f - \left(\frac{S_f^0}{S_f} \delta_f + \mu_f \right) I_f \right] \gamma^{1-\alpha} \\ & + R_{0,mf} \left[\left(1 - \frac{S_m^0}{S_m} \right) \mu_m (S_m^0 - S_m) + S_m^0 \bar{\lambda}_m - \left(\frac{S_m^0}{S_m} \delta_m + \mu_m \right) I_m \right] \gamma^{1-\alpha} \\ = & \left[-\frac{\mu_f}{S_f} (S_f^0 - S_f)^2 + \beta_{mf} I_m - (\delta_f + \mu_f) I_f \right] \gamma^{1-\alpha} \\ & + R_{0,mf} \left[\frac{\mu_m^0}{S_m} \mu_m (S_m^0 - S_m) + S_m^0 \bar{\lambda}_m - \left(\frac{S_m^0}{S_m} \delta_m \mu_m \right) I_m \right] \gamma^{1-\alpha} \\ = & \left[-\frac{\mu_f}{S_f} (S_f^0 - S_f)^2 - R_{0,mf} \frac{\mu_m}{S_m} (S_m^0 - S_m)^2 \right. \\ & \left. + \left(\beta_{mf} - R_{0,mf} (\delta_m + \mu_m) \right) I_m + \left(R_{0,mf} \beta_{fm} - (\delta_f + \mu_f) \right) I_f \right] \gamma^{1-\alpha} \\ = & \left[-\frac{\mu_f}{S_f} (S_f^0 - S_f)^2 - R_{0,mf} \frac{\mu_m}{S_m} (S_m^0 - S_m)^2 + (\delta_f + \mu_f)(R_0^2 - 1) I_f \right] \gamma^{1-\alpha} \end{aligned}$$

Since $R_0 \leq 1$, we have $\mathbf{D}_t^\alpha V \leq 0$ and $\mathbf{D}_t^\alpha V = 0$ if and only if $S_f(t) = S_f^0$, $I_f(t) = I_f^0$, $S_m(t) = S_m^0$, and $I_m(t) = I_m^0$. Therefore, by LaSalle's invariance principle [50,51], the disease-free equilibrium E^0 is globally asymptotically stable when $R_0 \leq 1$.

□

The endemic equilibrium was derived in [20]. We present the results here for completeness. Theorem 4 provides the endemic equilibrium E^*, which is same as the ODE case. Then, Theorem 5 shows the local stability conditions of the endemic equilibrium E^*.

Theorem 4. *When $R_0 > 1$, a unique endemic equilibrium $E^* = (S_f^*, I_f^*, S_m^*, I_m^*)$ exists and is given by*

$$S_f^* = \frac{N_m^*(\delta_m + \mu_m) + N_f^*\beta_{fm}}{p_f N_m^*(\delta_m + \mu_m)}, I_f = \frac{R_0^2 - 1}{p_f}. \tag{3.5}$$

$$S_m^* = \frac{N_f^*(\delta_f + \mu_f) + N_m^*\beta_{mf}}{p_m N_f^*(\delta_f + \mu_f)}, I_m = \frac{R_0^2 - 1}{p_m}. \tag{3.6}$$

and

$$p_f = \frac{R_0^2}{N_f^*} + \frac{\beta_{fm}}{N_m^*(\delta_m + \mu_m)}, p_m = \frac{R_0^2}{N_m^*} + \frac{\beta_{mf}}{N_f^*(\delta_f + \mu_f)} \tag{3.7}$$

$$N_f^* = \Lambda_f/\mu_f, N_m^* = \Lambda_m/\mu_m. \tag{3.8}$$

Theorem 5. *When $R_0 > 1$, the endemic equilibrium E^* is locally asymptotically stable.*

Proof. The Jacobian matrix of the systems (2.1)–(2.4) at the endemic equilibrium $E^* = (S_f^*, I_f^*, S_m^*, I_m^*)$ is evaluated as follows:

$$J(E^*) = \begin{bmatrix} j_{11} & j_{12} & j_{13} & 0 \\ j_{21} & j_{22} & 0 & j_{24} \\ j_{31} & j_{32} & j_{33} & 0 \\ j_{41} & j_{42} & 0 & j_{44} \end{bmatrix}$$

where

$$j_{11} = -\gamma^{\alpha-1}\left(\frac{\beta_{mf} I_m^* S_f^*}{N_f^{*2}} + (\delta_f + \mu_f)\right), j_{12} = \gamma^{\alpha-1}\frac{\beta_{mf} S_f^*}{N_f^*}, \tag{3.9}$$

$$j_{13} = \gamma^{\alpha-1}\left(\frac{\beta_{mf} I_m^*}{N_f^*} - \frac{\beta_{mf} I_m^* S_f^*}{N_f^{*2}}\right), j_{21} = \gamma^{\alpha-1}\frac{\beta_{fm} S_m^*}{N_m^*}, \tag{3.10}$$

$$j_{22} = -\gamma^{\alpha-1}\left(\frac{\beta_{fm} I_f^* S_m^*}{N_m^{*2}} + (\delta_m + \mu_m)\right), j_{24} = \gamma^{\alpha-1}\left(\frac{\beta_{fm} I_f^*}{N_m^*} - \frac{\beta_{fm} I_f^* S_m^*}{N_m^{*2}}\right), \tag{3.11}$$

$$j_{31} = \gamma^{\alpha-1}\left(\frac{\beta_{mf} I_m^* S_f^*}{N_f^{*2}} + \delta_f\right), j_{32} = -\gamma^{\alpha-1}\frac{\beta_{mf} S_f^*}{N_f^*}, \tag{3.12}$$

$$j_{33} = -\gamma^{\alpha-1}\left(\frac{\beta_{mf} I_m^*}{N_f^*} - \frac{\beta_{mf} I_m^* S_f^*}{N_f^{*2}} - \mu_f\right), j_{41} = -\gamma^{\alpha-1}\frac{\beta_{fm} S_m^*}{N_m^*}, \tag{3.13}$$

$$j_{42} = \gamma^{\alpha-1}\left(\frac{\beta_{fm} I_f^* S_m^*}{N_m^{*2}} + \delta_m\right), j_{44} = -\gamma^{\alpha-1}\left(\frac{\beta_{fm} I_f^*}{N_m^*} - \frac{\beta_{fm} I_f^* S_m^*}{N_m^{*2}} + \mu_m\right). \tag{3.14}$$

we then have

$$|J(E^*) - \lambda \mathbf{I}| = \begin{vmatrix} j_{11} - \lambda & j_{12} & j_{13} & 0 \\ j_{21} & j_{22} - \lambda & 0 & j_{24} \\ j_{31} & j_{32} & j_{33} - \lambda & 0 \\ j_{41} & j_{42} & 0 & j_{44} - \lambda \end{vmatrix}.$$

After addition of first row to the third and second to the last, we obtain

$$|J(E^*) - \lambda \mathbf{I}| = \begin{vmatrix} j_{11} - \lambda & j_{12} & j_{13} & 0 \\ j_{21} & j_{22} - \lambda & 0 & j_{24} \\ -\gamma^{\alpha-1}\mu_f - \lambda & 0 & -\gamma^{\alpha-1}\mu_f - \lambda & 0 \\ 0 & -\gamma^{\alpha-1}\mu_m - \lambda & 0 & -\gamma^{\alpha-1}\mu_m - \lambda \end{vmatrix}.$$

The characteristic equation is $(\lambda + \gamma^{\alpha-1}\mu_f)(\lambda + \gamma^{\alpha-1}\mu_m)(\lambda^2 + b\lambda + c)$, where

$$b = \gamma^{\alpha-1}\left(\delta_f + \mu_f + \delta_m + \mu_m + \frac{\beta_{fm} I_f^*}{N_m^*} + \frac{\beta_{mf} I_m^*}{N_f^*}\right) > 0, \tag{3.15}$$

$$c = \gamma^{\alpha-1}\left((\delta_f + \mu_f)(\delta_m + \mu_m) + (\delta_f + \mu_f)\frac{\beta_{fm} I_f^*}{N_m^*} + (\delta_m + \mu_m)\frac{\beta_{mf} I_m^*}{N_f^*}\right) > 0. \tag{3.16}$$

One can see that all eigenvalues of $J(E^*)$ have negative real parts. Therefore, the FDE systems (2.1)–(2.4) is stable by Theorem 1. □

4. Numerical simulations, data fitting, and identifiability analysis

4.1. Data source

HPV is widely recognized as a primary etiological factor for oropharyngeal cancer (OPC). Several studies have demonstrated a strong link between HPV infection, and the development of OPC [52–56]. Despite this strong connection, there are no yearly data on HPV's prevalence or incidence available for both genders. With this limitation, we use the OPC incidence data as a proxy for HPV-induced cancer data. This decision was informed by the fact that a significant proportion of OPCs in the United States and Turkey are attributable to HPV infection. According to a study by Damgacioglu et al. [57], OPC incidence has been rising, aligning with the increasing prevalence of HPV-related cases in the US. This rise in incidence directly reflects the upward trend in HPV-driven OPCs, making the available data on OPC a reasonable substitute. Therefore, we employed the OPC incidence data from [58]. While the data do not explicitly provide HPV-related cases, the strong connection between HPV and OPC incidence means that trends in OPC incidence are likely to reflect trends in HPV infection. Throughout the subsequent analysis, our systems (2.1)–(2.4) is modified by using the per capita cancer rate parameters η_f and η_m to substitute the cancer data as a proxy for HPV data such as $c_f = \eta_f I_f$ and $c_m = \eta_m I_m$.

As a result, due to the unavailability of direct, yearly HPV data for both genders (i.e., female and male) we used OPC incidence data as an alternative source. The established link between HPV and OPC, provides a reliable and scientifically valid basis for our study.

4.2. Structural identifiability

Understanding the relationship between the model's parameters and observable data is essential for accurate predictions. For this reason, structural identifiability is a useful tool to ensure whether a model's parameters can be uniquely determined from the available data. For structural identifiability purposes in an epidemiological model, input refers to the mode parameters such as transmission rates and output refers the measurable data, such as the number of infected individuals, and recruitment and mortality rates. In the models (2.1)–(2.4), the given outputs are the observed yearly cancer data $\eta_f I_f$ and $\eta_m I_m$, the fractional-order derivative α, the auxiliary parameter γ, and the exit rate from sexually active individuals μ_f and μ_m. To analyze structural identifiability there are some software and packages such as GenSSI [59], SIAN [60], and DAISY [61]. However, to the best of our knowledge, the software developed for structural identifiability only works with ODE systems but not FDE systems. In order to analyze structural identifiability, we employ the differential algebra approach. This technique involves analyzing the relationships between the output equations and the model's parameters through algebraic manipulations and derivatives. Considering the fractional-order equation systems (2.1)–(2.4), we have

$$\gamma^{\alpha-1}\mathbf{D}_t^\alpha S_f(t) = \Lambda_f - \lambda_f S_f + \delta_f I_f - \mu_f S_f, \tag{4.1}$$
$$\gamma^{\alpha-1}\mathbf{D}_t^\alpha I_f(t) = \lambda_f S_f - \delta_f I_f - \mu_f I_f, \tag{4.2}$$
$$\gamma^{\alpha-1}\mathbf{D}_t^\alpha S_m(t) = \Lambda_m - \lambda_m S_m + \delta_m I_m - \mu_m S_m, \tag{4.3}$$
$$\gamma^{\alpha-1}\mathbf{D}_t^\alpha I_m(t) = \lambda_f S_m - \delta_m I_m - \mu_m I_m \tag{4.4}$$

$$y_1 = \eta_f I_f$$
$$y_2 = \eta_m I_m$$

All parameters are considered to be divided by $\gamma^{\alpha-1}$. Male and female data on cancer $\alpha, \gamma, \mu_f, \mu_m$ are given as well as $S_f(0)$ and $S_m(0)$. We assume that the given outputs are

$$y_1 = \eta_f I_f$$
$$y_2 = \eta_m I_m.$$

$$\mathbf{D}_t^\alpha S_f = \Lambda_f - \frac{\beta_{mf}}{\eta_m}\frac{y_2 S_f}{N_f} + \frac{\delta_f}{\eta_f} y_1 - \mu_f S_f \tag{4.5}$$

$$\mathbf{D}_t^\alpha y_1 = \frac{\eta_f}{\eta_m}\frac{\beta_{mf} y_2 S_f}{N_f} - (\delta_f + \mu_f) y_1 \tag{4.6}$$

Using S_f from (4.6). First, we rewrite (4.6) as

$$\mathbf{D}_t^\alpha y_1 = \frac{\eta_f}{\eta_m}\frac{\beta_{mf} y_2 S_f}{S_f + \frac{1}{\eta_f} y_1} - (\delta_f + \mu_f) y_1.$$

Solving for S_f, we have

$$\mathbf{D}_t^\alpha y_1\left(S_f+\frac{1}{\eta_f}y_1\right)=\frac{\eta_f}{\eta_m}\beta_{mf}y_2S_f-(\delta_f+\mu_f)y_1\left(S_f+\frac{1}{\eta_f}y_1\right)$$
$$\left(\mathbf{D}_t^\alpha y_1-\frac{\eta_f}{\eta_m}\beta_{mf}y_2+(\delta_f+\mu_f)y_1\right)S_f=-\mathbf{D}_t^\alpha y_1\frac{1}{\eta_f}y_1-\frac{1}{\eta_f}(\delta_f+\mu_f)y_1^2$$
$$S_f=\frac{-\mathbf{D}_t^\alpha y_1\frac{1}{\eta_f}y_1-\frac{1}{\eta_f}(\delta_f+\mu_f)y_1^2}{\mathbf{D}_t^\alpha y_1-\frac{\eta_f}{\eta_m}\beta_{mf}y_2+(\delta_f+\mu_f)y_1}$$

Substituting in (4.5), we have

$$\mathbf{D}_t^\alpha S_f=\Lambda_f-\frac{1}{\eta_f}\left(\mathbf{D}_t^\alpha y_1+(\delta_f+\mu_f)y_1\right)+\frac{\delta_f}{\eta_f}y_1-\mu_f\frac{-\mathbf{D}_t^\alpha y_1\frac{1}{\eta_f}y_1-\frac{1}{\eta_f}(\delta_f+\mu_f)y_1^2}{\mathbf{D}_t^\alpha y_1-\frac{\eta_f}{\eta_m}\beta_{mf}y_2+(\delta_f+\mu_f)y_1}$$

Taking a common denominator, we have

$$\begin{aligned}\left(\mathbf{D}_t^\alpha y_1-\frac{\eta_f}{\eta_m}\beta_{mf}y_2+(\delta_f+\mu_f)y_1\right)\mathbf{D}_t^\alpha S_f&=\Lambda_f\left(\mathbf{D}_t^\alpha y_1-\frac{\eta_f}{\eta_m}\beta_{mf}y_2+(\delta_f+\mu_f)y_1\right)\\&-\frac{1}{\eta_f}\left(\mathbf{D}_t^\alpha y_1+(\delta_f+\mu_f)y_1\right)\left(\mathbf{D}_t^\alpha y_1-\frac{\eta_f}{\eta_m}\beta_{mf}y_2+(\delta_f+\mu_f)y_1\right)\\&+\frac{\delta_f}{\eta_f}y_1\left(\mathbf{D}_t^\alpha y_1-\frac{\eta_f}{\eta_m}\beta_{mf}y_2+(\delta_f+\mu_f)y_1\right)+\mu_f\left(\mathbf{D}_t^\alpha y_1\frac{1}{\eta_f}y_1+\frac{1}{\eta_f}(\delta_f+\mu_f)y_1^2\right)\end{aligned}\tag{4.7}$$

Rewriting (4.7) as

$$\begin{aligned}\left(\mathbf{D}_t^\alpha y_1-\frac{\eta_f}{\eta_m}\beta_{mf}y_2+(\delta_f+\mu_f)y_1\right)\mathbf{D}_t^\alpha S_f&=\Lambda_f\left(\mathbf{D}_t^\alpha y_1-\frac{\eta_f}{\eta_m}\beta_{mf}y_2+(\delta_f+\mu_f)y_1\right)\\&-\frac{1}{\eta_f}\left(\mathbf{D}_t^\alpha y_1+(\delta_f+\mu_f)y_1\right)\left(\mathbf{D}_t^\alpha y_1-\frac{\eta_f}{\eta_m}\beta_{mf}y_2+(\delta_f+\mu_f)y_1\right)\\&+\frac{\delta_f+\mu_f}{\eta_f}y_1\left(\mathbf{D}_t^\alpha y_1+(\delta_f+\mu_f)y_1\right)-\frac{\delta_f}{\eta_m}\beta_{mf}y_1y_2\end{aligned}\tag{4.8}$$

$$\begin{aligned}\left(\mathbf{D}_t^\alpha y_1-\frac{\eta_f}{\eta_m}\beta_{mf}y_2+(\delta_f+\mu_f)y_1\right)\mathbf{D}_t^\alpha S_f&=\Lambda_f\left(\mathbf{D}_t^\alpha y_1-\frac{\eta_f}{\eta_m}\beta_{mf}y_2+(\delta_f+\mu_f)y_1\right)\\&-\frac{1}{\eta_f}\left(\mathbf{D}_t^\alpha y_1+(\delta_f+\mu_f)y_1\right)\left(\mathbf{D}_t^\alpha y_1-\frac{\eta_f}{\eta_m}\beta_{mf}y_2\right)\\&-\frac{1}{\eta_f}\mathbf{D}_t^\alpha y_1(\delta_f+\mu_f)y_1+\frac{\delta_f+\mu_f}{\eta_f}y_1\mathbf{D}_t^\alpha y_1-\frac{\delta_f}{\eta_m}\beta_{mf}y_1y_2\end{aligned}\tag{4.9}$$

From (4.9), we have the following results:

- The coefficient in front of $\mathbf{D}_t^\alpha y_1$ is Λ_f, which implies that Λ_f is identifiable.

- The coefficient in front of y_2 is $\Lambda_f \frac{\eta_f}{\eta_m}\beta_{mf}$. This implies that $\frac{\eta_f}{\eta_m}\beta_{mf}$ is identifiable.
- The coefficient in front of y_1 is $\Lambda_f(\delta_f + \mu_f)$, which implies that $(\delta_f + \mu_f)$ identifiable and then δ_f is identifiable.
- The coefficient in front of $(\mathbf{D}_t^\alpha y_1)^2$ is $-\frac{1}{\eta_f}$, which implies that η_f is identifiable.
- The coefficient in front of $y_1 \mathbf{D}_t^\alpha y_1$ is $-\frac{1}{\eta_f}(\delta_f + \mu_f)$, which is identifiable.
- Since $\frac{\eta_f}{\eta_m}\beta_{mf}$ is identifiable and η_f is identifiable, $\frac{\beta_{mf}}{\eta_m}$ is identifiable.
- From the male compartments, we can see that if η_m is identifiable, then β_{mf} is identifiable.
- From the male compartments, we can see that δ_m, β_{fm} and Λ_m are identifiable.
- We assume that $c_f(0)$ and $c_m(0)$ are given with the data. Since η_f and η_m are identifiable, this implies that $I_f(0)$ and $I_m(0)$ are identifiable.

Thus, all parameters are identifiable.

4.3. Data fitting

In our analysis, we utilized the lip, oral cavity, and pharynx cancer incidence data from [58], which covers the years 1998 to 2017. During the data fitting procedure of our FDE systems (2.1)–(2.4), we modify the model by using the per capita cancer rate parameters η_f and η_m to substitute for the cancer data as a proxy for HPV data.

The initial points during parameter estimation are based on HPV's prevalence in Turkey (about 4.39% of women in the general population [5, 62]) and in the US (about 3.9% [7] in the studied population) in the available data [58].

Table 4. Fitted values of parameters for the ODE case with ranges and units.

Parameter	Fitted value		Range		Unit	Source
symbols	TR	US	TR	US		
β_{fm}	0.7299	0.7299	[0.5896,0.7299]	[0.5896,0.7299]	1/year	[20]
β_{mf}	2.6594	2.6594	[2.6594,4.5373]	[2.6594,4.5373]	1/year	[20]
δ_f	0.988235	1.00778	[12/13.3,12/7.7]	[12/13.3,12/7.7]	1/year	[20]
δ_m	1.55844	1.55844	[12/7.7,12/6.2]	[12/7.7,12/6.2]	1/year	[20]
Λ_f	53064	131644	[8525,53064]	[69665,131644]	person/year	Calibrated
Λ_m	24888	130112	[18843,84123]	[54161,130112]	person/year	Calibrated
μ_f	0.02	0.02	[1/50,1/18]	[1/50,1/18]	1/year	Calibrated
μ_m	0.0166667	0.0166667	[1/60,1/18]	[1/60, 1/18]	1/year	Calibrated
η_f	0.000324394	0.000805618	[0,1]	[0,1]	1/year	Calibrated
η_m	0.00143185	0.00323644	[0,1]	[0,1]	1/year	Calibrated
γ	Fixed	Fixed	[0.5,1.5]	[0.5,1.5]	1/year	Calibrated

During data fitting, the fractional derivative order α is considered to be $0.5, 0.7, 0.9$, and 1 in order to understand the behavior of the system, while the order of the derivative starting from the middle of the interval ($\alpha = 0.5$) and converging to the ODE case ($\alpha = 1$). In Tables 5 and 6, the fitted values of parameters for the fractional-order derivatives $\alpha = 0.5, 0.7, 0.9$, and 1 (ODE case) are presented for the data of Turkey and the USA, respectively.

During the data fitting process, the ranges of the parameters except δ_f and δ_m are calibrated by the authors. δ_f and δ_m lower bounds and upper bounds are depend on the clearance of the virus from the

body, which is 7.7–13.3 months for females and 6.2–7.7 months for males. So the range of the recovery rate parameter is considered to be [12/13.3,12/7.7] for females and [12/7.7,12/6.3] for males [20]. Λ_f and Λ_m are calculated by the yearly difference of the time series for the newly susceptible population. The ranges of μ_f and μ_m are determined by the sexually active ages of females (18 to 50 years) and males (18 to 60 years). In Table 4, fitted values, ranges and units of the estimated parameters for the ODE case of the models (2.1)–(2.4) are presented. The same ranges are taken into account for the fractional order cases.

Table 5. Parameter estimation for the model with the data from Turkey with various fractional orders α with $\gamma = 1$.

Parameter	$\alpha = 0.5$	$\alpha = 0.7$	$\alpha = 0.9$	$\alpha = 1$(ODE case)
β_{fm}	0.7299	0.7299	0.7299	0.7299
β_{mf}	2.96266	2.6594	2.6594	2.6594
δ_f	0.902256	0.915851	0.969585	0.988235
δ_m	1.55844	1.55844	1.55844	1.55844
Λ_f	53064	53064	53064	53064
Λ_m	84123	84123	33472	24888
μ_f	0.02	0.02	0.02	0.02
μ_m	0.0166667	0.0166667	0.0166667	0.0166667
η_f	0.000324394	0.000389178	0.000397595	0.000805618
η_m	0.0012195	0.00136604	0.00141622	0.00143185
Squared error	7.4176748×10^3	6.9240679×10^3	6.8350600×10^3	6.8303498×10^3

Table 6. Parameter estimation for the model with the data from the USA with various fractional orders α with $\gamma = 1$.

Parameter	$\alpha = 0.5$	$\alpha = 0.7$	$\alpha = 0.9$	$\alpha = 1$(ODE case)
β_{fm}	0.7299	0.7299	0.7299	0.7299
β_{mf}	2.76303	2.6594	2.6594	2.6594
δ_f	0.902256	0.944859	0.992505	1.00778
δ_m	1.55844	1.55844	1.55844	1.55844
Λ_f	131644	131644	131644	131644
Λ_m	130112	130112	130112	130112
μ_f	0.02	0.02	0.02	0.02
μ_m	0.0166667	0.0166667	0.0166667	0.0166667
η_f	0.000732271	0.000785911	0.000801525	0.000805618
η_m	0.0030047	0.00313745	0.0032165	0.00323644
Squared error	6.7102802×10^5	5.8192133×10^5	5.7122526×10^5	5.8945856×10^5

According to Table 5, the error values show that the data for Turkey fits well to our models (2.1)–(2.4). Moreover, the data fit better as the order of the derivative increases. The best fit is obtained when $\alpha = 1$, which is the ODE case. However, the data for the USA fits relatively worse to our model. It can be seen in Table 6 that, surprisingly, the fractional-order derivative model has better fit than the ODE model for this case. There would be an optimal fractional-order derivative which might fit best to our

model for parameter estimation with the US data.

Graphs of the data and the fitted values for incidences during the parameter estimation process of the models (2.1)–(2.4) for the fractional-order derivatives $\alpha = 0.5, 0.7, 0.9$, and 1 (the ODE case) are presented in Figure 2(a),(b) for the data of Turkey and in Figure 2(c),(d) for the data of the USA.

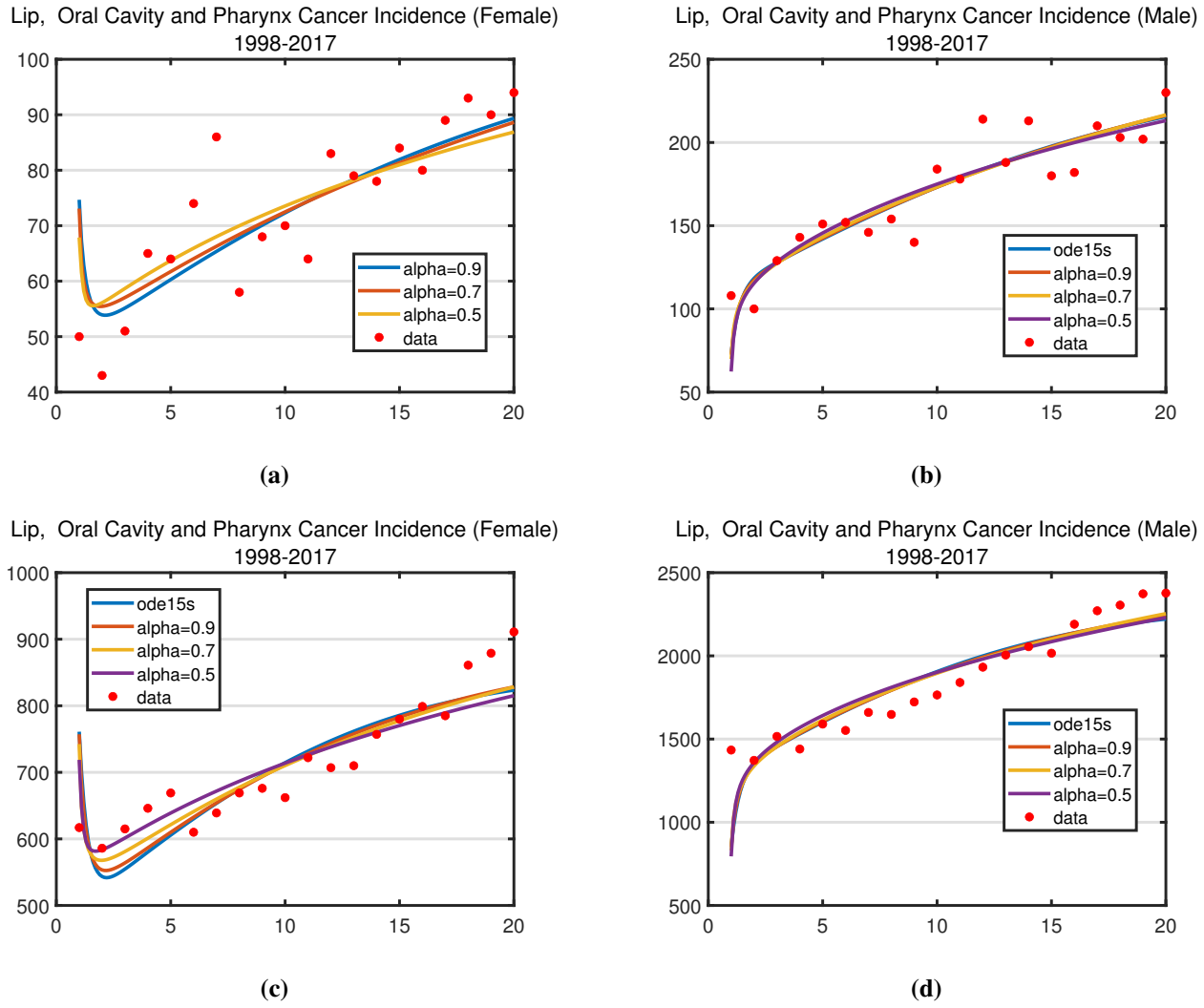

Figure 2. Lip, oral cavity and pharyngeal cancer incidence and the estimated values for various fractional orders α: (a) Females (Turkey), (b) males (Turkey), (c) females (USA), and (d) males (USA).

Error graphs of the parameter estimations of the models (2.1)–(2.4) for the fractional-order derivatives $\alpha = 0.5, 0.7, 0.9$, and 1 (ODE case) are presented in Figure 3(a),(b) for the data of Turkey and in Figure 3(c),(d) for the data from the USA. We see that the residuals for Turkey are relatively random with signifies a good fit. The residuals for the USA have more pattern to them, which signifies that the models (2.1)–(2.4) is not a good model to fit for the US data.

4.4. *Practical identifiability*

In mathematical modeling, determining whether the estimated parameters are practically identifiable is essential for the generation of reliable conclusions. Unlike structural identifiability, which is a theoretical property of the model's equations, practical identifiability reflects the ability to recover the parameter values from noisy or limited real-world data.

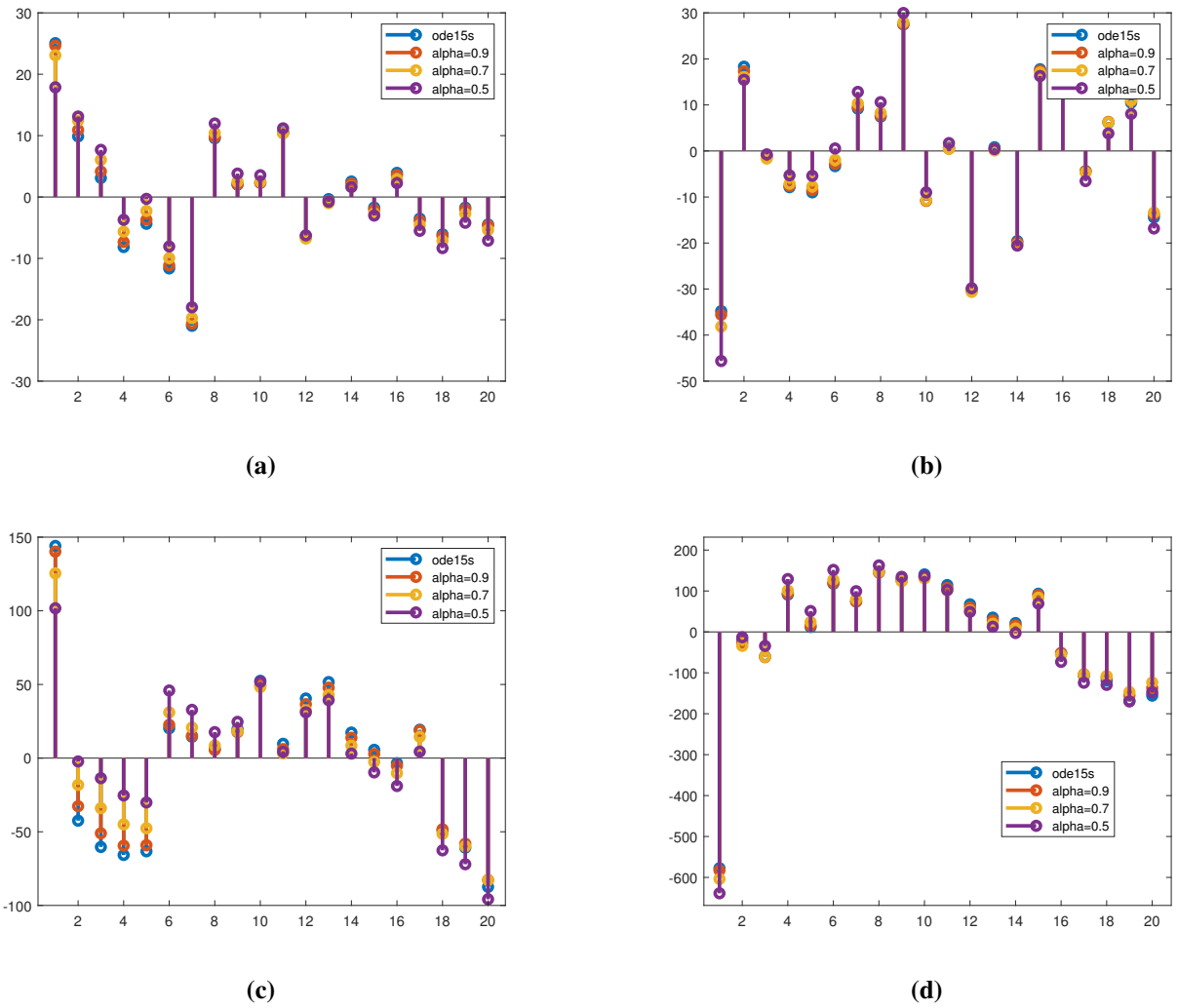

Figure 3. Residual error plots for parameter estimation: (a) Females (Turkey), (b) males (Turkey), (c) females (USA), and (d) males (USA).

One of the most widely used techniques to evaluate practical identifiability is the Monte Carlo simulation approach. In this method, synthetic data are generated using known parameter values, often perturbed with various noise levels to simulate experimental variability. Subsequently, these datasets are used to re-estimate the model's parameters under identical conditions to those applied in real data fitting. Here, by repeating this process 1000 times, one can assess how consistently and accurately the parameters can be recovered. Monte Carlo simulations also allow the exploration of identifiability under diverse scenarios, including varying noise levels, which provides insights into how the noise influences the parameters' recoverability.

A key metric derived from the simulations is the average relative error (ARE), defined as the average of the relative differences between the true (estimated) and predicted (simulated) parameter values across all runs. The ARE formula [63] is expressed as follows

$$ARE(y^{(j)}) = 100\% \frac{1}{n} \sum_{i=1}^{n} \frac{|\hat{y}^{(j)} - y_i^{(j)}|}{\hat{y}^{(j)}},$$

where n is the number of observations, $y^{(j)}$ is the j^{th} parameter in the parameter set $\mathbf{y}$, $\hat{y}^{(j)}$ is the j^{th} parameter in the true parameter set $\hat{\mathbf{y}}$, and $y_i^{(j)}$ is the j^{th} parameter in the estimated parameter set $\mathbf{y_i}$. Low ARE values indicate that the model can reliably estimate the parameter despite data noise, suggesting strong practical identifiability. Conversely, high ARE values suggest that the parameter estimates are unstable or unreliable under realistic conditions, even if the model is structurally identifiable.

By incorporating Monte Carlo simulation and ARE analysis into the model evaluation, one can make relatively more informed judgments about the reliability of parameter estimation and the limitations of the model's predictions. We refer the interested reader to the articles in [63–65] for more details and applications on practical identifiability and Monte Carlo simulations.

In Tables 7–10 and in Tables 11–14, the ARE values of the estimated parameters based on the data of Turkey and the United States are presented, respectively, for various noise levels. Regarding Tables 7–10, the ARE values as a result of Monte Carlo simulations for estimated parameters of the model for Turkey are increasing while the noise level is increasing. The parameters Λ_f, Λ_m, β_{fm}, δ_f, δ_m, μ_f, η_f, and η_m are found to be practically identifiable but μ_m is unidentifiable. When the estimated parameters for $\alpha = 0.9$ are considered, we get one additional unidentifiable parameter. Regarding the values of Table 9, all parameters are practically identifiable except Λ_m and μ_m.

Table 7. ARE scores of the estimated parameters with the data from Turkey for various noise levels obtained by Monte Carlo simulations with $\alpha = 0.5$ and $\gamma = 1$.

Parameter symbols	Noise level 0%	5%	10%	30%	Practical identifiablity
Λ_f	0.0000	5.3708	8.6546	15.4611	Identifiable
Λ_m	0.0008	6.4325	9.9017	13.7766	Identifiable
β_{fm}	0.0001	1.8865	4.4215	15.0651	Identifiable
β_{mf}	0.0000	0.1725	0.4531	1.5630	Identifiable
δ_f	0.0000	0.4083	1.2525	5.9809	Identifiable
δ_m	0.0001	0.3007	0.7627	2.3537	Identifiable
μ_f	0.0004	5.7315	11.8067	30.2894	Unidentifiable
μ_m	0.0002	20.9468	36.0220	53.1178	Unidentifiable
η_f	0.0001	2.2890	4.9356	14.3058	Identifiable
η_m	0.0001	1.5051	3.0660	8.4115	Identifiable

According to Tables 11–14, the ARE values as a result of Monte Carlo simulations for the estimated parameters of the model for the United States are increasing while noise level is increasing similar to the estimated parameters of the model for Turkey. The parameters Λ_f, Λ_m, β_{fm}, δ_f, δ_m, μ_f, η_f, and η_m are found to be practically identifiable but μ_m is unidentifiable. When the estimated parameters for

Table 8. ARE scores of the estimated parameters with the data from Turkey for various noise levels obtained by Monte Carlo simulations with $\alpha = 0.7$ and $\gamma = 1$.

Parameter symbols	Noise level 0%	5%	10%	30%	Practical identifiablity
Λ_f	0.0000	2.0214	4.5223	11.0498	Identifiable
Λ_m	0.0002	3.9232	6.5889	12.2428	Identifiable
β_{fm}	0.0000	1.5518	3.4489	11.5782	Identifiable
β_{mf}	0.0000	0.3961	0.8178	1.6896	Identifiable
δ_f	0.0001	0.7001	1.3658	4.5249	Identifiable
δ_m	0.0001	0.6656	1.1201	2.6014	Identifiable
μ_f	0.0000	3.6285	7.1266	22.3766	Identifiable
μ_m	0.0000	28.3245	40.1846	52.5601	Unidentifiable
η_f	0.0001	1.4992	3.3575	10.8419	Identifiable
η_m	0.0000	1.2232	2.3726	6.9880	Identifiable

Table 9. ARE scores of the estimated parameters with the data from Turkey for various noise levels obtained by Monte Carlo simulations with $\alpha = 0.9$ and $\gamma = 1$.

Parameter symbols	Noise level 0%	5%	10%	30%	Practical identifiablity
Λ_f	0.0019	3.7664	3.9149	2.7051	Identifiable
Λ_m	0.0059	66.3397	90.0768	95.8879	Unidentifiable
β_{fm}	0.0000	1.8125	2.7798	6.8307	Identifiable
β_{mf}	0.0000	0.8002	1.0839	1.9960	Identifiable
δ_f	0.0002	0.9535	1.5373	3.6222	Identifiable
δ_m	0.0001	0.6211	1.6082	3.2469	Identifiable
μ_f	0.0003	3.8325	4.8639	7.5374	Identifiable
μ_m	0.0005	14.6455	28.3930	44.3606	Unidentifiable
η_f	0.0001	1.5645	2.3651	6.5894	Identifiable
η_m	0.0000	1.2586	2.3259	4.8459	Identifiable

Table 10. ARE scores of the estimated parameters with the data from Turkey for various noise levels obtained by Monte Carlo simulations with the ODE case and $\gamma = 1$.

Parameter symbols	Noise level 0%	5%	10%	30%	Practical identifiablity
Λ_f	0.0001	4.4030	7.5031	14.7573	Identifiable
Λ_m	0.0003	123.7630	140.0282	144.7305	Unidentifiable
β_{fm}	0.0000	2.8570	5.4321	12.8927	Identifiable
β_{mf}	0.0000	0.8807	1.7129	2.7853	Identifiable
δ_f	0.0001	2.3763	4.3149	8.4200	Identifiable
δ_m	0.0001	1.2266	2.3685	4.2238	Identifiable
μ_f	0.0000	7.5466	11.5528	29.3930	Unidentifiable
μ_m	0.0002	48.3851	63.3200	74.9234	Unidentifiable
η_f	0.0001	2.9137	5.7884	15.7299	Identifiable
η_m	0.0000	2.7643	5.2089	14.2253	Identifiable

$\alpha = 0.5$ is considered, we get one additional unidentifiable parameter. Regarding the values of the Table 11, all parameters are practically identifiable except μ_f and μ_m.

Table 11. ARE scores of the estimated parameters with the data from the USA for various noise levels obtained by Monte Carlo simulations with $\alpha = 0.5$ and $\gamma = 1$.

Parameter symbols	Noise level 0%	5%	10%	30%	Practical identifiablity
Λ_f	0.0020	6.2176	7.2575	9.7850	Identifiable
Λ_m	0.0032	7.4773	9.2046	11.4839	Identifiable
β_{fm}	0.0001	2.5826	6.6122	20.5448	Identifiable
β_{mf}	0.0000	0.2499	0.7317	2.0175	Identifiable
δ_f	0.0000	0.7083	2.5353	10.5501	Identifiable
δ_m	0.0001	0.4551	1.2982	3.3665	Identifiable
μ_f	0.0001	11.8281	23.3776	40.8648	Unidentifiable
μ_m	0.0001	35.1421	49.3047	68.0446	Unidentifiable
η_f	0.0001	2.6903	6.1233	16.3601	Identifiable
η_m	0.0001	1.5181	3.0204	7.8575	Identifiable

4.5. Numerical simulations

In this section, we perform numerical simulations with the models (2.1)–(2.4). For numerical solutions of the studied system, we employ the Adams-Bashforth-Moulton method as the predictor–corrector technique described in [66, 67]. All computations for both fractional-order and integer-order derivatives were performed with MATLAB R2024a software. The ODE results are obtained by using the built-in function ode15s. The parameters of the models (2.1)–(2.4) are estimated for each α separately with respect to the various values of γ to demonstrate the effect of the fractional-order derivative α and the auxiliary parameter γ. Parameter estimation procedure is applied

Table 12. ARE scores of the estimated parameters with the data from the USA for various noise levels obtained by Monte Carlo simulations with $\alpha = 0.7$ and $\gamma = 1$.

Parameter	Noise level				Practical
symbols	0%	5%	10%	30%	identifiablity
Λ_f	0.0000	2.4397	4.2028	11.0498	Identifiable
Λ_m	0.0009	4.5237	7.2618	12.2428	Identifiable
β_{fm}	0.0000	1.6637	3.6781	11.5782	Identifiable
β_{mf}	0.0000	0.5377	1.0444	1.6896	Identifiable
δ_f	0.0001	0.9875	1.9557	4.5249	Identifiable
δ_m	0.0001	0.8345	1.5805	2.6014	Identifiable
μ_f	0.0000	4.1102	10.7829	22.3766	Identifiable
μ_m	0.0002	32.7623	49.3506	52.5601	Unidentifiable
η_f	0.0001	1.4490	3.1657	10.8419	Identifiable
η_m	0.0000	1.2267	2.3581	6.9880	Identifiable

Table 13. ARE scores of the estimated parameters with the data from the USA for various noise levels obtained by Monte Carlo simulations with $\alpha = 0.9$ and $\gamma = 1$.

Parameter	Noise level				Practical
Symbols	0%	5%	10%	30%	identifiablity
Λ_f	0.0000	1.1933	2.2831	5.4781	Identifiable
Λ_m	0.0000	2.7699	4.0831	8.8883	Identifiable
β_{fm}	0.0000	1.1538	2.3411	6.7446	Identifiable
β_{mf}	0.0000	0.5044	1.0096	2.0685	Identifiable
δ_f	0.0001	0.7499	1.6157	4.6879	Identifiable
δ_m	0.0001	0.6934	1.3097	3.0564	Identifiable
μ_f	0.0000	1.6987	3.5629	14.0842	Identifiable
μ_m	0.0000	14.3608	27.3303	53.4523	Unidentifiable
η_f	0.0001	1.1518	2.2940	6.7112	Identifiable
η_m	0.0000	1.0123	2.0169	5.5726	Identifiable

Table 14. ARE scores of the estimated parameters with the data from the USA for various noise levels obtained by Monte Carlo simulations with the ODE case and $\gamma = 1$.

Parameter symbols	Noise level 0%	5%	10%	30%	Practical identifiablity
Λ_f	0.0000	2.9881	4.7638	9.1660	Identifiable
Λ_m	0.0002	5.5895	8.6188	11.7082	Identifiable
β_{fm}	0.0000	2.3580	4.6391	13.3258	Identifiable
β_{mf}	0.0000	0.9587	1.7883	3.0354	Identifiable
δ_f	0.0001	2.3826	4.4529	9.6597	Identifiable
δ_m	0.0001	1.4871	2.4571	3.6584	Identifiable
μ_f	0.0001	4.6076	11.4209	32.8894	Unidentifiable
μ_m	0.0001	32.3906	50.4136	68.8536	Unidentifiable
η_f	0.0001	2.7737	5.5017	16.2387	Identifiable
η_m	0.0000	2.7379	5.2146	14.4387	Identifiable

for the datasets of both countries, namely Turkey and the USA. In Figure 4, we present numerical solutions of the systems (2.1)–(2.4) with a fixed $\gamma = 1$ for various fractional-order derivatives with respect to the estimated parameters for the dataset of Turkey. Numerical simulations of the models (2.1)–(2.4) for various values of γ represented in Figures 5–7 for $\alpha = 0.5$, $\alpha = 0.7$, and $\alpha = 0.9$, respectively. Similarly, numerical simulations are presented in Figures 8–11 with the estimated parameters regarding the dataset of the USA for various fractional orders as well. When we consider the behavior of the model with parameters obtained for the data from Turkey, we obtain interesting results. First, if we focus on Figure 4(c) and Figure 7(c), one can see that the behavior of the fractional-order models (2.1)–(2.4) with $\alpha = 0.9$ and $\gamma = 0.5$ approaches that of the ODE model. A similar situation exists in Figure 7(a),(b),(d) for the corresponding model solutions of the ODE model. Moreover, when α converges to $\alpha = 1$, in all cases, the distinction between the model's solutions regarding the value of γ decreases and γ loses its effect, as expected. Similar behavior can be seen in Figures 9–11, which demonstrate the behavior of the model with the estimated parameters for the data from the USA. It can be concluded from Figures 9–11 that when α converges to $\alpha = 1$, the model's solutions get closer with respect to the value of γ. So the auxiliary parameter γ loses its effect dramatically. While the models (2.1)–(2.4) adjusted to the data of Turkey converges to ODE model with $\alpha = 0.9$ and $\gamma = 0.5$, the fractional-order model with parameters obtained from the data from the USA converges to the ODE model with the same order $\alpha = 0.9$ but a different $\gamma = 1.5$. In general, it can be seen that the fractional-order models (2.1)–(2.4) fits better with the data of the USA than with the data of Turkey. Finally, irregularities in the graph of Figure 4(c) may be caused by the value of the parameter μ_m which was found to be unidentifiable during the practical identifiability analysis presented in Table 8.

5. Discussion and conclusions

In this study, we proposed a fractional-order differential equation model to investigate the gender-specific dynamics of HPV transmission. Due to the unavailability of consistent, yearly HPV incidence data disaggregated by gender, we utilized OPC incidence data as a proxy, justified by the

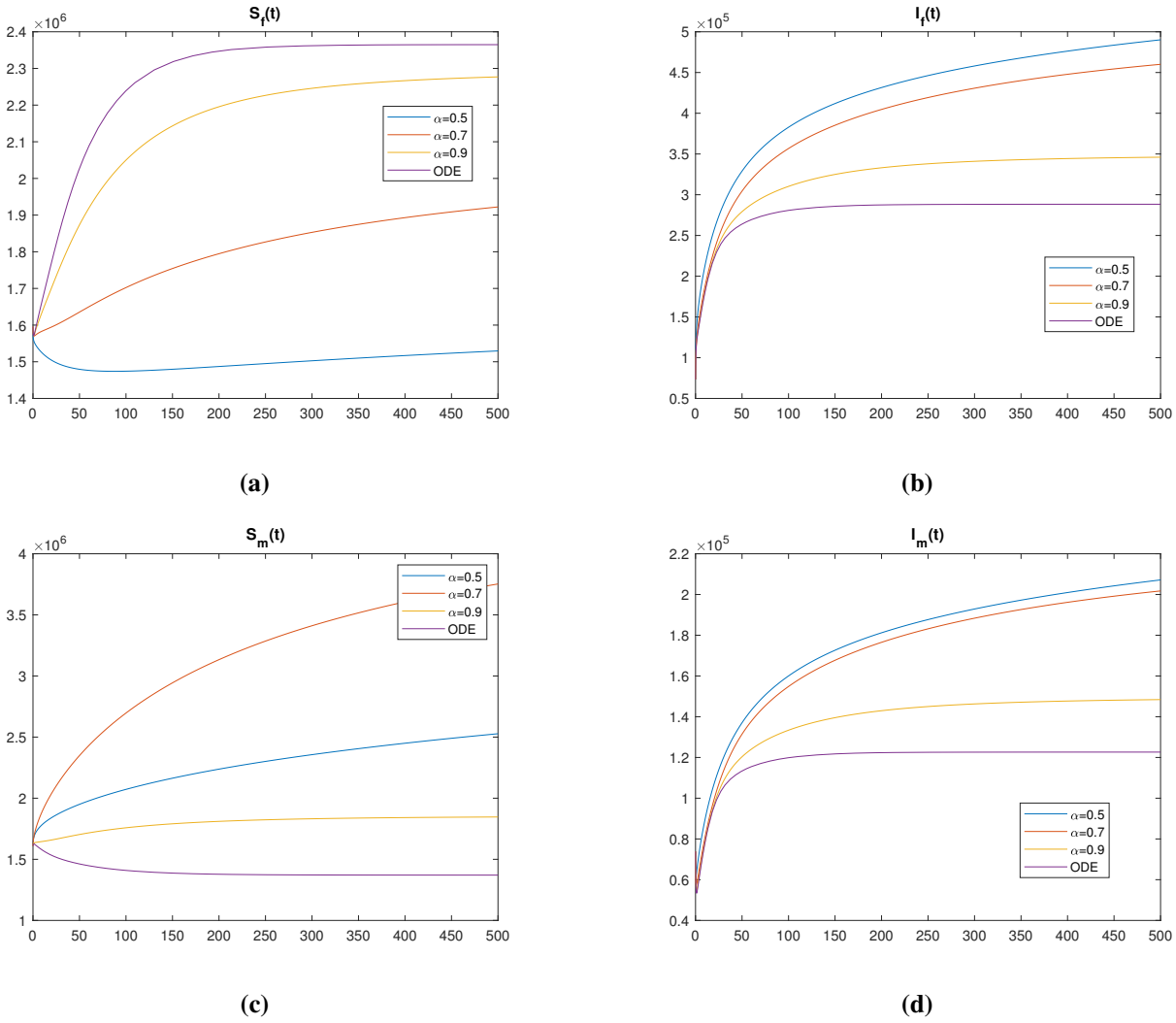

Figure 4. Numerical solutions for the systems (2.1)–(2.4) with the estimated parameters regarding the data from Turkey for $\gamma = 1$: (a) $S_f(t)$, (b) $I_f(t)$, (c) $S_m(t)$, (d) $I_m(t)$.

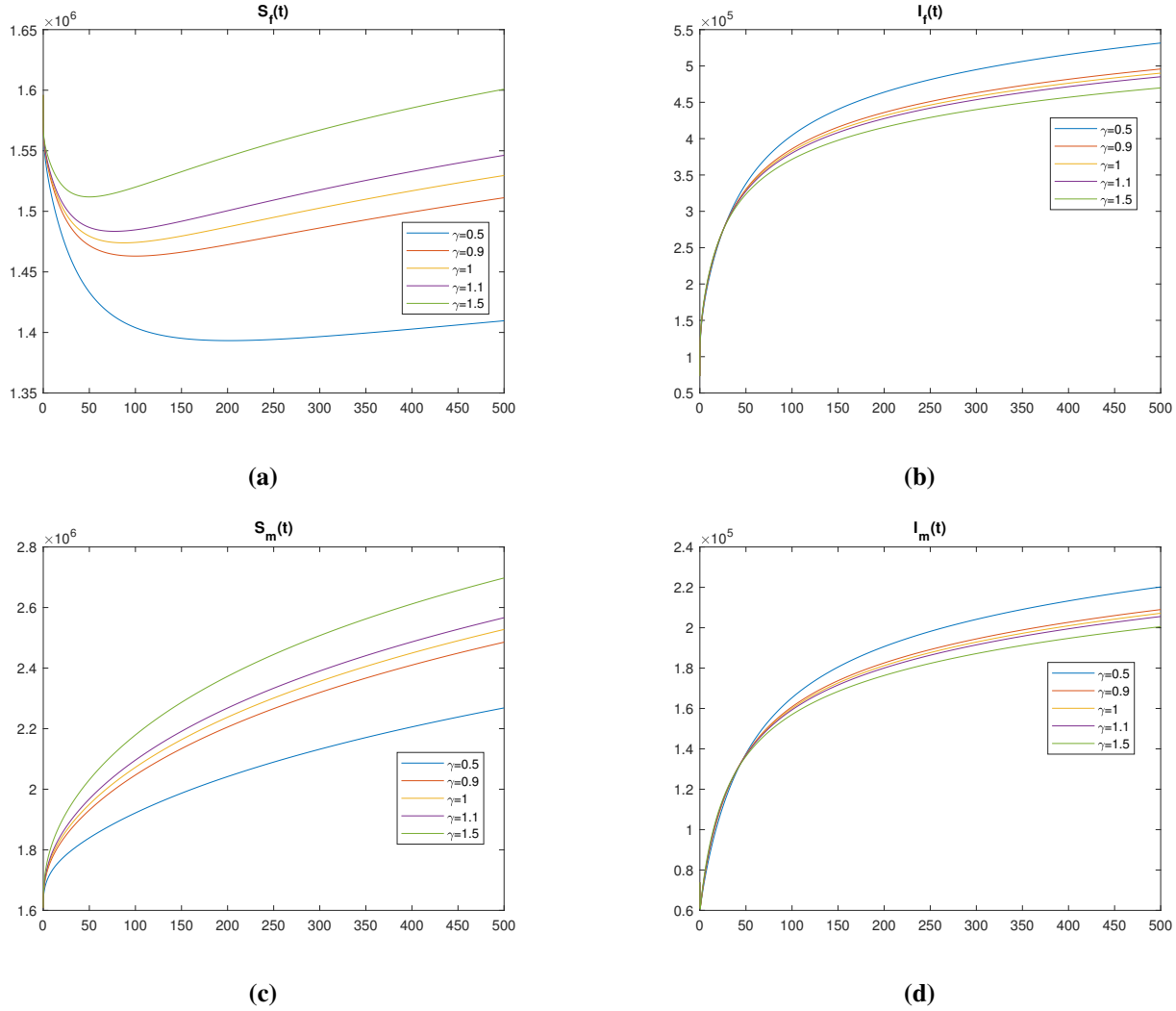

Figure 5. Numerical solutions for the systems (2.1)–(2.4) with the estimated parameters regarding the data from Turkey for various values of γ and $\alpha = 0.5$: (a) $S_f(t)$, (b) $I_f(t)$, (c) $S_m(t)$, (d) $I_m(t)$.

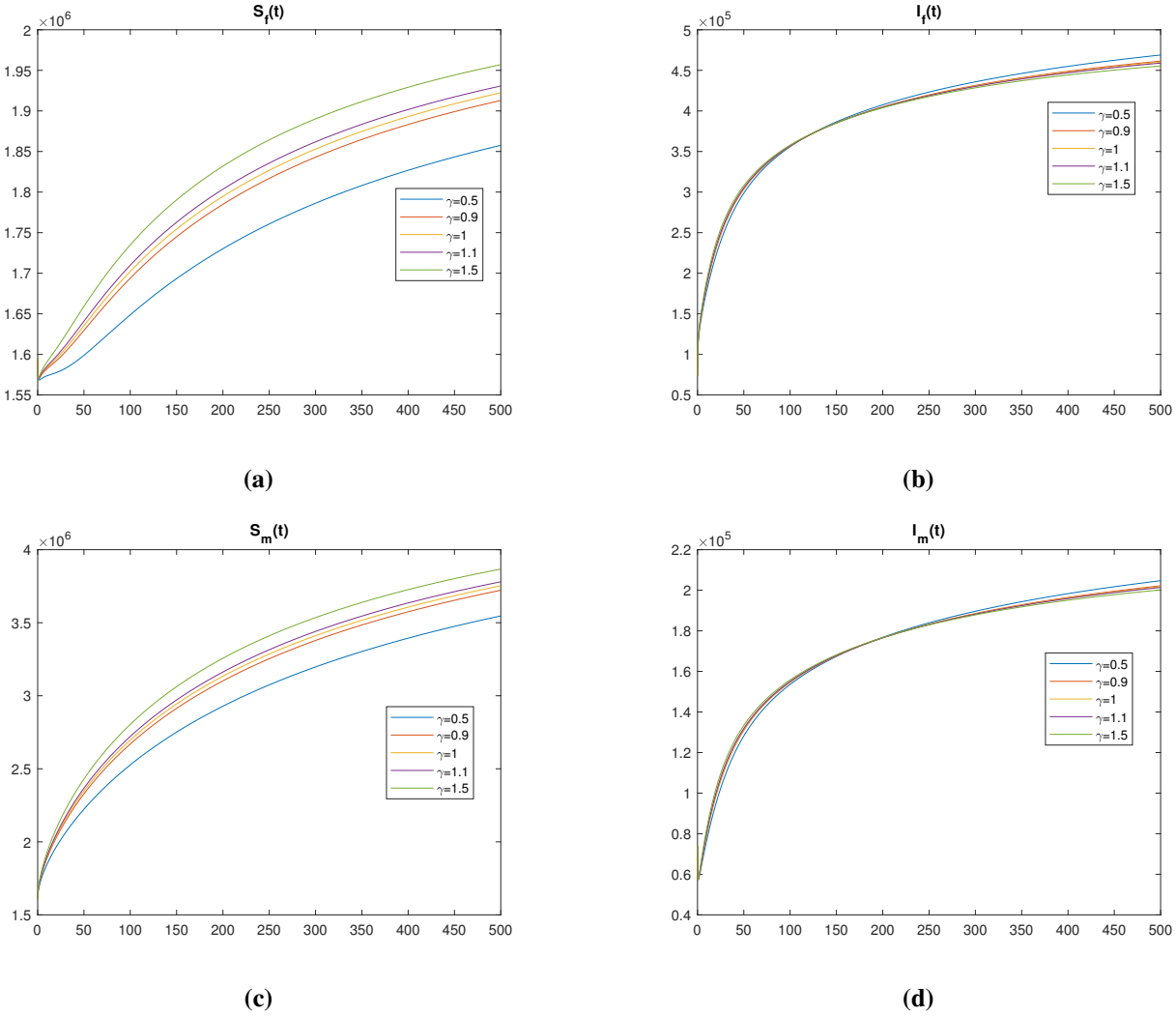

Figure 6. Numerical solutions for the systems (2.1)–(2.4) with the estimated parameters regarding the data from Turkey for various values of γ and $\alpha = 0.7$: (a) $S_f(t)$, (b) $I_f(t)$, (c) $S_m(t)$, (d) $I_m(t)$.

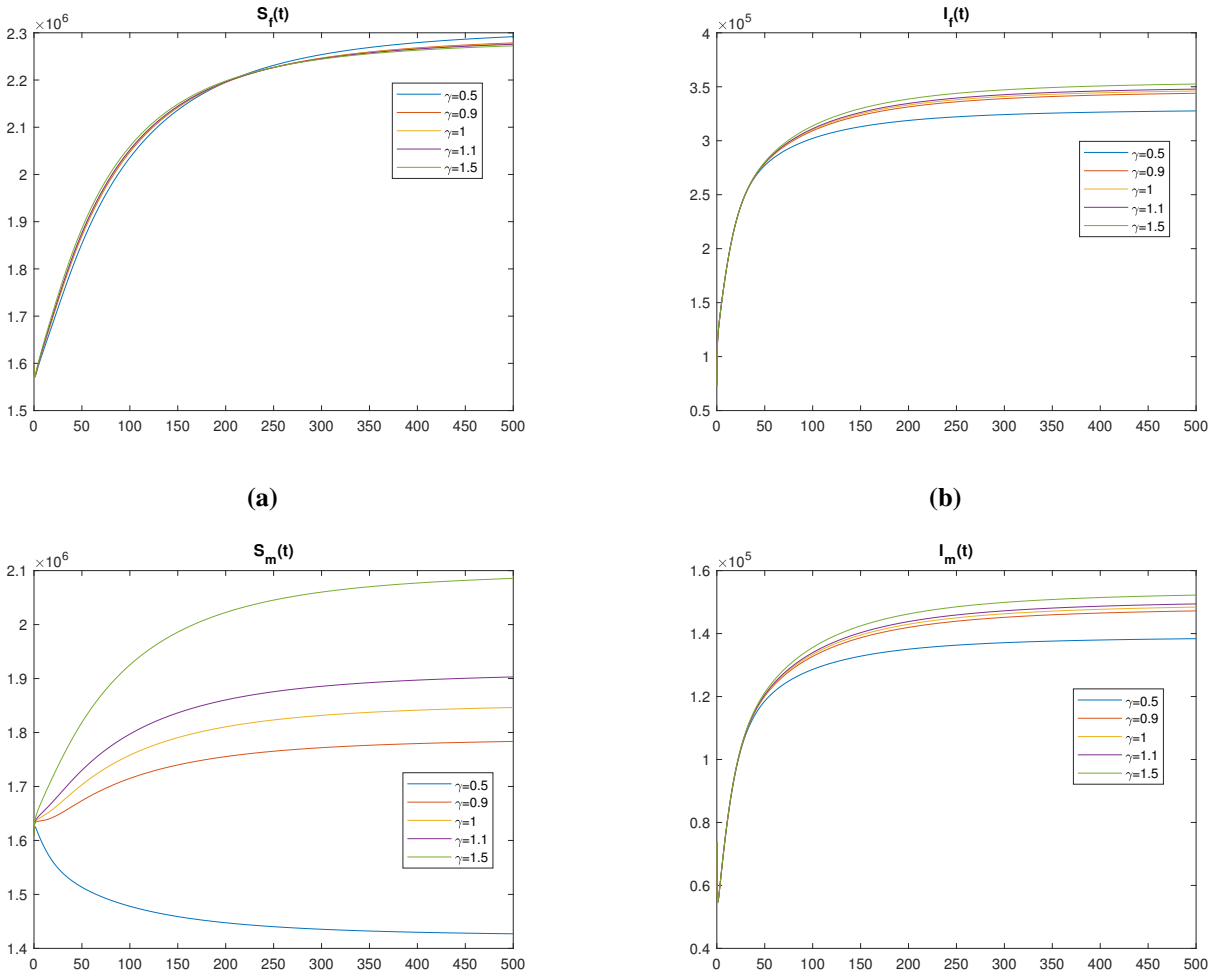

Figure 7. Numerical solutions for the systems (2.1)–(2.4) with the estimated parameters regarding the data from Turkey for various values of γ and $\alpha = 0.9$: (a) $S_f(t)$, (b) $I_f(t)$, (c) $S_m(t)$, (d) $I_m(t)$.

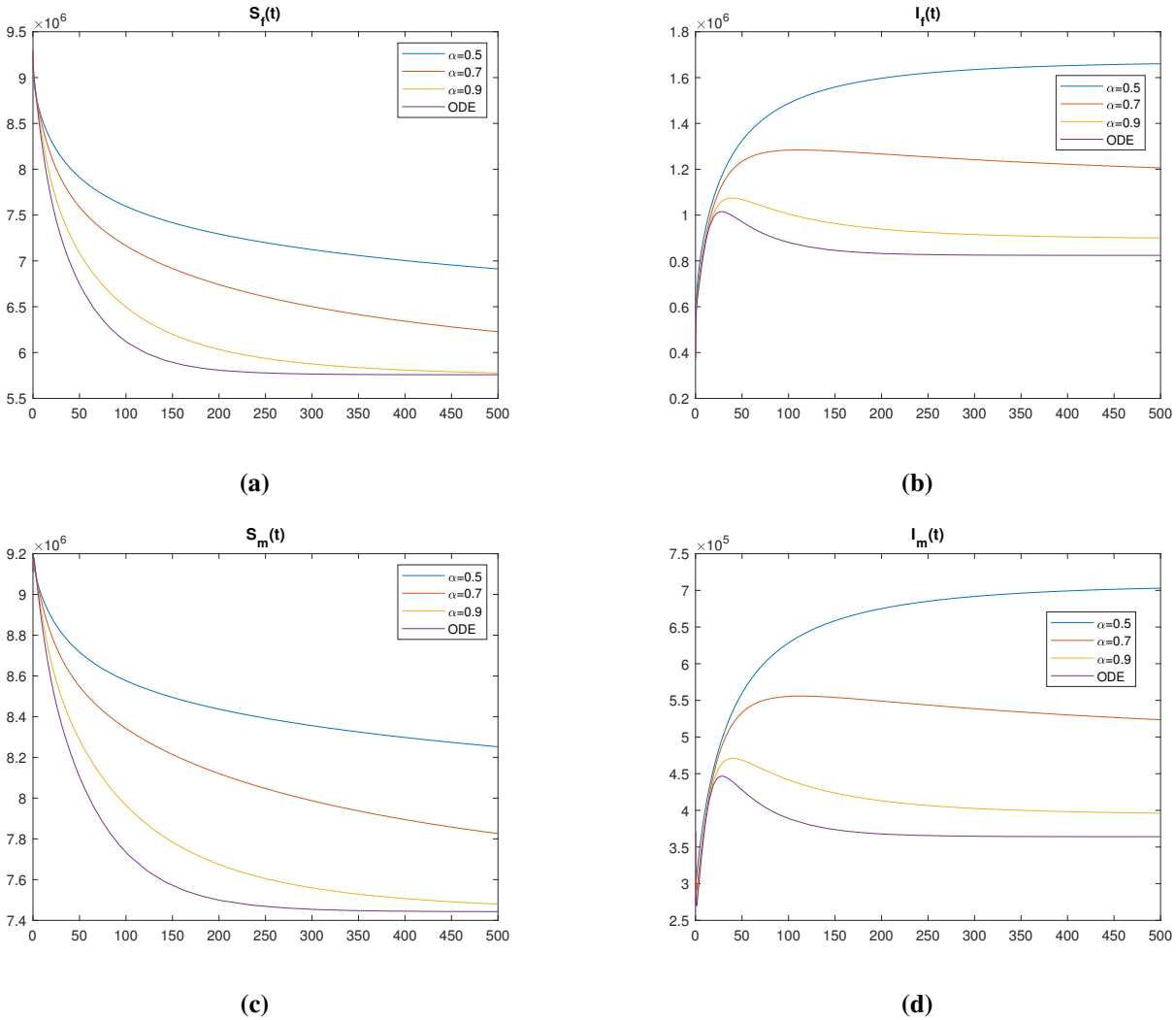

Figure 8. Numerical solutions for the systems (2.1)–(2.4) with the estimated parameters regarding the data from the USA for $\gamma = 1$: (a) $S_f(t)$, (b) $I_f(t)$, (c) $S_m(t)$, (d) $I_m(t)$.

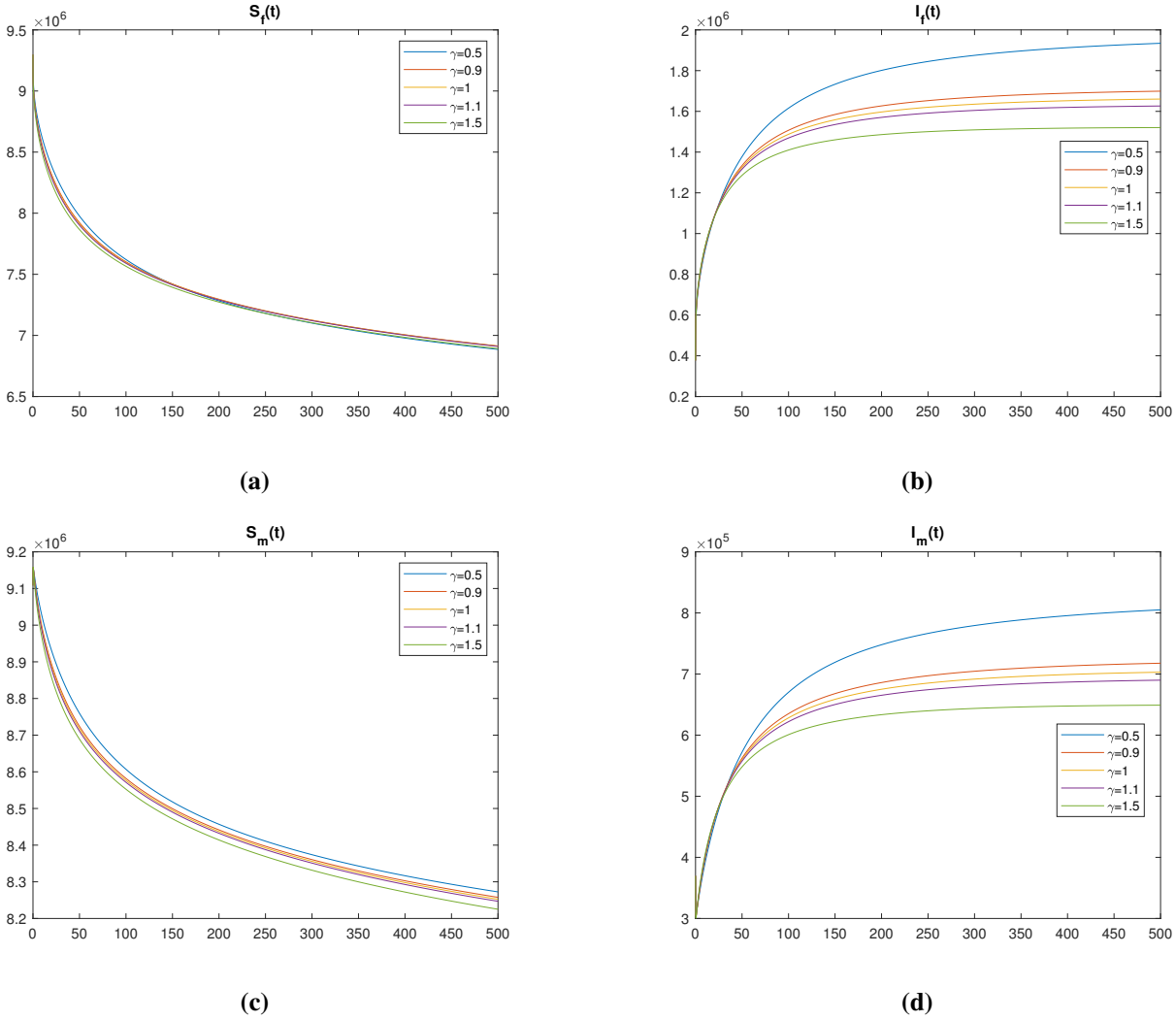

Figure 9. Numerical solutions for the systems (2.1)–(2.4) with the estimated parameters regarding the data from the USA for various values of γ and $\alpha = 0.5$: (a) $S_f(t)$, (b) $I_f(t)$, (c) $S_m(t)$, (d) $I_m(t)$.

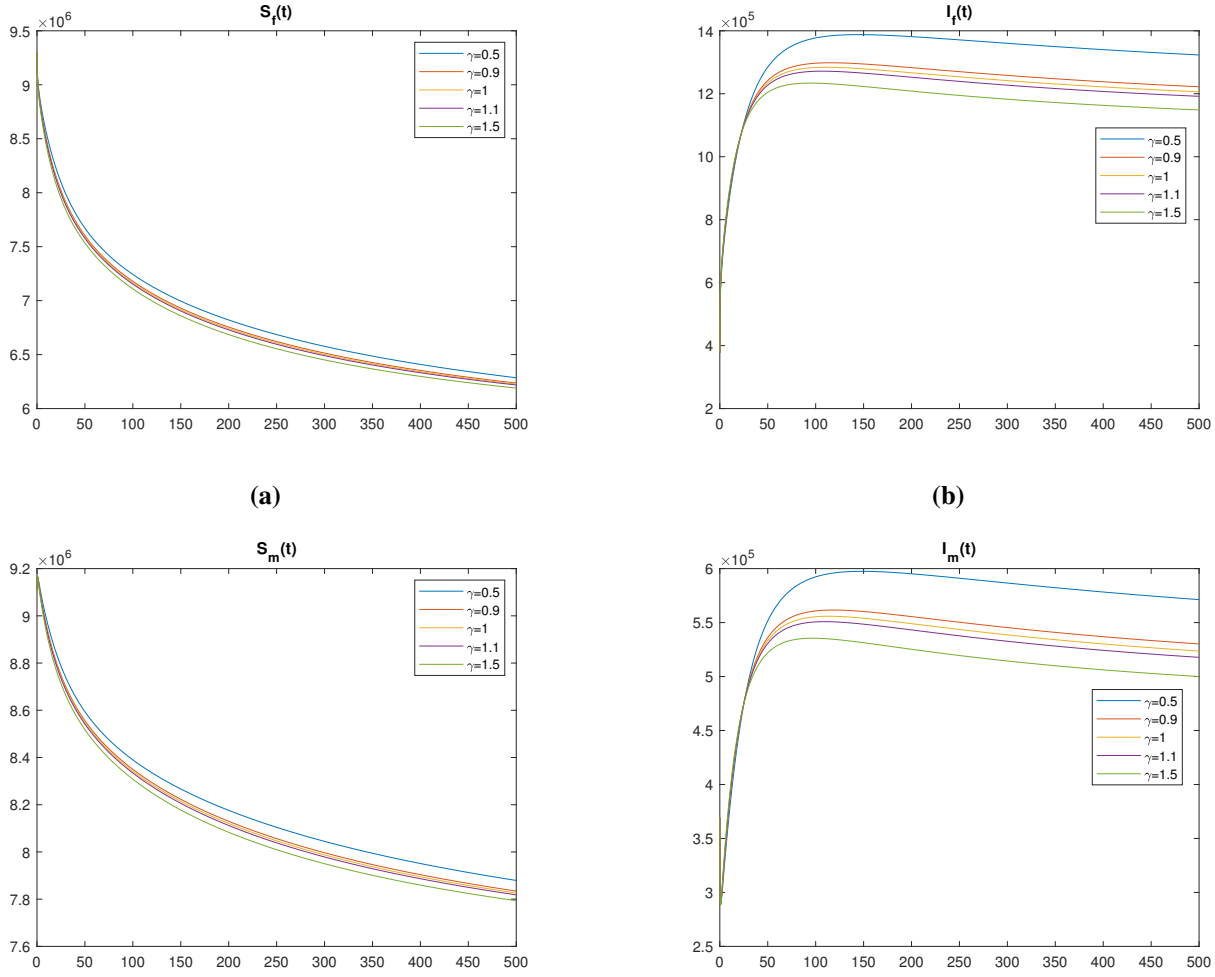

Figure 10. Numerical solutions for the systems (2.1)–(2.4) with the estimated parameters regarding the data from the USA for various values of γ and $\alpha = 0.7$: (a) $S_f(t)$, (b) $I_f(t)$, (c) $S_m(t)$, (d) $I_m(t)$.

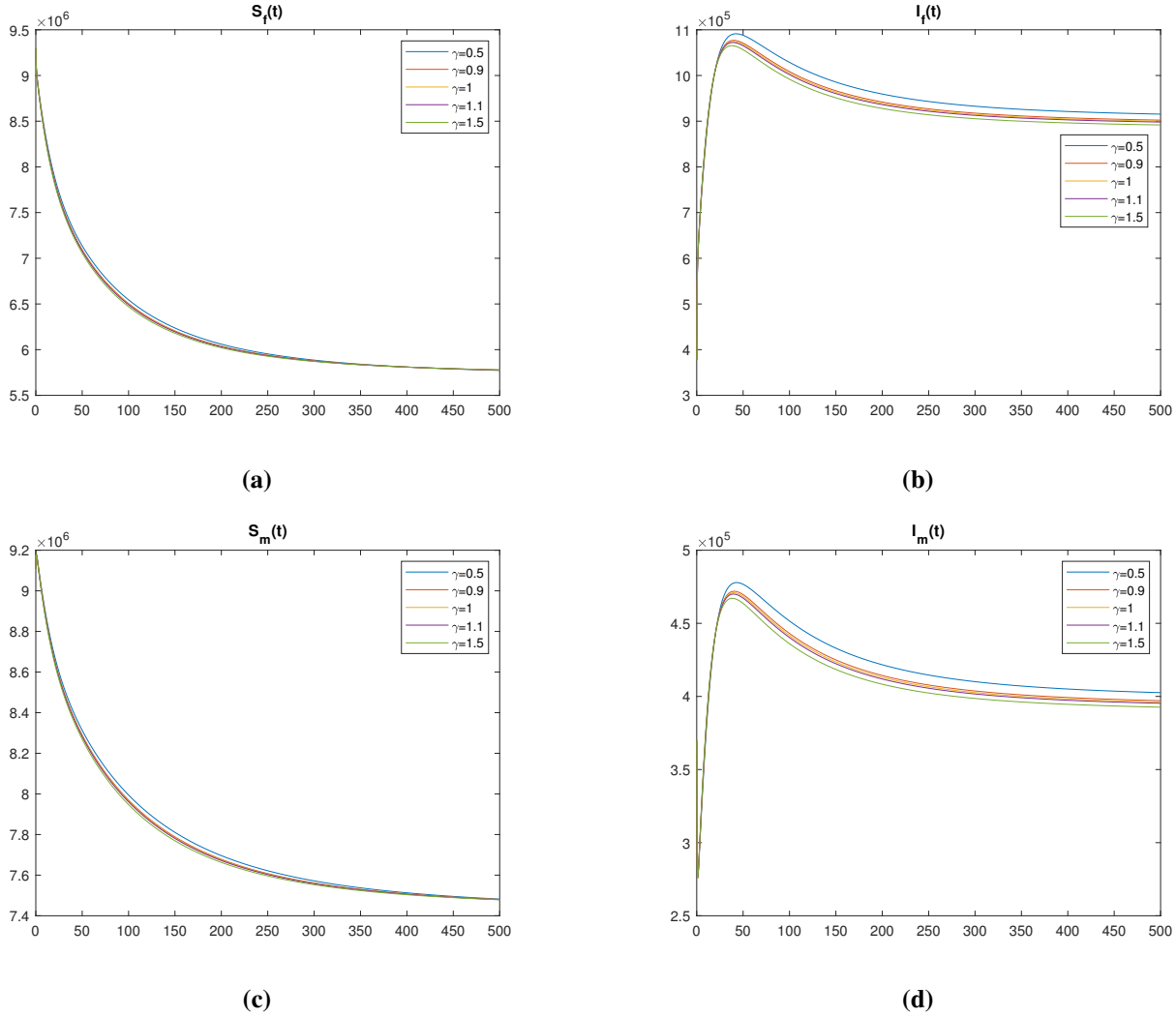

Figure 11. Numerical solutions for the systems (2.1)–(2.4) with the estimated parameters regarding the data from the USA for various values of γ and $\alpha = 0.9$: (a) $S_f(t)$, (b) $I_f(t)$, (c) $S_m(t)$, (d) $I_m(t)$.

strong epidemiological association between HPV infection and OPC, particularly in the United States. While indirect, this approach enabled us to calibrate and validate the model with meaningful real-world data.

The model formulation included a comprehensive theoretical analysis. We derived the disease-free equilibrium (DFE) and endemic equilibrium (EE) points and computed the basic reproduction number R_0, a key threshold parameter characterizing the transmission potential of the virus. Stability conditions for the equilibrium points were also established, showing that the DFE is locally asymptotically stable when $R_0 < 1$ and globally asymptotically stable when $R_0 \leq 1$, and the EE is stable when $R_0 > 1$. These results provide critical insight into the long-term behavior of the system under different epidemiological scenarios and intervention thresholds.

We conducted a structural identifiability analysis using the differential algebra approach, confirming that the key transmission parameters—including the cross-gender transmission rates β_{fm} and β_{mf}—are identifiable. This theoretical finding supports the validity of the model's structure for parameter estimation from the given data.

In modeling the spread of infectious diseases, fractional-order models can capture the long-range memory effects related to disease progression. The fractional order can be interpreted as a measure of how significant these memory effects are [68]. Data fitting to OPC incidence from Turkey and the US revealed that the model fits better to the data for Turkey when the derivative order α equaled 1 (classical ODE), while for the US, the best fit occurred for fractional-order models (e.g., $\alpha = 0.9$). This suggests that fractional-order dynamics, which capture memory and hereditary effects, may better reflect disease progression and reporting patterns in some populations. Moreover, Turkish data have a higher level of noise, which might have made the memory effect disappear in the noise.

We also examined practical identifiability through Monte Carlo simulations under various noise levels. Most parameters—including recruitment, transmission, and progression rates—showed good identifiability, as indicated by the low ARE values. However, certain parameters such as the male exit rate μ_m were poorly identifiable, especially at higher noise levels or specific fractional orders, limiting predictive confidence for some outputs.

Numerical simulations further illustrated the model's dynamic behavior across varying values of the fractional derivative order α and the auxiliary parameter γ. As α approached 1, the influence of γ diminished, and the system's behavior converged toward the ODE case. Interestingly, for the US data, the model with $\alpha = 0.9$ and $\gamma = 1.5$ closely approximated the classical model, while for Turkey, a similar convergence was observed for $\gamma = 0.5$. These results confirm the sensitivity of the model to fractional effects and highlight its flexibility in capturing diverse epidemic trajectories.

Finally, the irregularities observed in certain simulation outputs, particularly for Turkey, were attributed to parameters identified as practically unidentifiable—such as μ_m—demonstrating the importance of identifiability analysis in interpreting the model's reliability.

In conclusion, this work presents a robust mathematical framework for modeling gender-specific HPV transmission dynamics using fractional-order derivatives. The theoretical results, including equilibrium analysis and reproduction number computation, combined with structural and practical identifiability studies, provide strong support for the model's validity. Despite limitations due to proxy data use and some unidentifiable parameters, the model offers valuable insights into HPV transmission patterns. Future work may focus on integrating vaccination strategies, refining data sources, and exploring optimal control policies, thereby enhancing the model's utility for public

health decision-making. To strengthen our outcomes, we may compare through simulations not only with ODEs but also with systems based on different fractional derivative definitions.

Data availability

The dataset on OPC incidence is available as open data at https://gco.iarc.fr/overtime.

Use of AI tools declaration

The authors declare they have not used artificial intelligence (AI) tools in the creation of this article.

Acknowledgement

This paper was prepared during the first author's visit to University of Florida, where they were a postdoctoral researcher. Veysel Fuat Hatipoğlu would like to acknowledge the generous financial support from the TÜBİTAK (the Scientific and Technological Research Council of Türkiye) 2219 International Postdoctoral Research Fellowship Program, Grant Project 1059B192300058. The author is also grateful to the University of Florida for their generous hospitality and for providing the facilities. The authors would like to thank Necibe Tuncer and Osman Raşit Işık for their support. The authors would like to thank the anonymous reviewers for their helpful comments and feedback, which have significantly improved the manuscript.

Conflict of interest

The authors declare there is no conflict of interest.

References

1. *HPV and Cancer, National Cancer Institute*. Avaiable from: https://www.cancer.gov/about-cancer/causes-prevention/risk/infectious-agents/hpv-and-cancer.
2. *Sexually Transmitted Infections*. Avaiable from: https://www.cdc.gov/sti/about/about-genital-hpv-infection.html.
3. V. Hancer, M. Buyukdogan, I. Bylykbashi, B. Oksuz, M. Acar, Prevalence of human papilloma virus types in Turkish and Albanian women, *J. Cytol.*, **35** (2018), 252–254. https://doi.org/10.4103/JOC.JOC_162_17
4. R. M. Lewis, J. Laprise, J. Gargano, E. Unger, T. Querec, H. Chesson, et al., Estimated prevalence and incidence of disease-associated human papillomavirus types among 15-to 59-year-olds in the United States, *Sex. Transm. Dis.*, **48** (2021), 273–277. https://doi.org/10.1097/OLQ.0000000000001356
5. *Human Papillomavirus and Related Cancers, Fact Sheet 2023, ICO/IARC Information Centre on HPV and Cancer Fact Sheet 2023*. Avaiable from:https://hpvcentre.net/statistics/reports/TUR_FS.pdf.

6. A. Bayram, Y. Derici, N. Yilmaz, S. Hanci, N. Agus, M. Sirin, et al., Prevalence of high-risk human papillomavirus in women from Turkey, *Clin. Obstet. Gynecol. Reprod. Med.*, **1** (2015), 84–86. https://doi.org/10.15761/COGRM.1000122

7. *HPV and Related Cancers, ICO/IARC Information Center on HPV and Cancer, Fact Sheet 2023*. Avaiable from:https://hpvcentre.net/statistics/reports/USA_FS.pdf.

8. S. Lee, A. Tameru, A mathematical model of human papillomavirus (HPV) in the United States and its impact on cervical cancer, *J. Cancer*, **3** (2012), 262–268. https://doi.org/10.7150/jca.4161

9. A. Sado, Mathematical modeling of cervical cancer with HPV transmission and vaccination, *Sci. J. Appl. Mat. Stat.*, **7** (2019), 21–25. https://doi.org/10.11648/j.sjams.20190702.13

10. K. Zhang, X. Wang, H. Liu, Y. Ji, Q. Pan, Y. Wei, et al., Mathematical analysis of a human papillomavirus transmission model with vaccination and screening, *Math. Biosci. Eng.*, **17** (2020), 5449–5476. https://doi.org/10.3934/mbe.2020294

11. E. J. Dasbach, E. H. Elbasha, R. P. Insinga, Mathematical models for predicting the epidemiologic and economic impact of vaccination against human papillomavirus infection and disease, *Epidemiol. Rev.*, **28** (2006), 88–100. https://doi.org/10.1093/epirev/mxj006

12. T. Malik, J. Reimer, A. Gumel, E. H. Elbasha, S. Mahmud, The impact of an imperfect vaccine and pap cytology screening on the transmission of human papillomavirus and occurrence of associated cervical dysplasia and cancer, *Math. Biosci. Eng.*, **10** (2013), 1173–1205. https://doi.org/10.3934/mbe.2013.10.1173

13. H. D. Desta, G. T. Tilahun, T. M. Tolasa, M. G. Geleso, Mathematical model of human papillomavirus (HPV) dynamics with double-dose vaccination and its impact on cervical cancer, *Discrete Dyn. Nat. Soc.*, **2024** (2024), 9971859. https://doi.org/10.1155/ddns/9971859

14. C. Liu, H. Liu, X. Zhu, X. Lin, Q. Zhang, Y. Wei, Dynamic analysis of human papillomavirus transmission model under vaccine intervention: A case study of cervical cancer patients from Hungary, *Adv. Cont. Discr. Mod.*, **2024** (2024), 36. https://doi.org/10.1186/s13662-024-03838-z

15. E. H. Elbasha, Global stability of equilibria in a two-sex HPV vaccination model, *Bull. Math. Biol.*, **70** (2008), 894–909. https://doi.org/10.1007/s11538-007-9283-0

16. A. Omame, R. Umana, D. Okuonghae, S. Inyama, Mathematical analysis of a two-sex human papillomavirus (HPV) model, *Int. J. Biomath.*, **11** (2018), 1850092. https://doi.org/10.1142/S1793524518500924

17. O. Sharomi, T. Malik, A model to assess the effect of vaccine compliance on human papillomavirus infection and cervical cancer, *Appl. Math. Modell.*, **47** (2017), 528–550. https://doi.org/10.1016/j.apm.2017.03.025

18. S. Gao, M. Martcheva, H. Miao, L. Rong, A dynamic model to assess human papillomavirus vaccination strategies in a heterosexual population combined with men who have sex with men, *Bull. Math. Biol.*, **83** (2021), 1–36. https://doi.org/10.1007/s11538-020-00830-y

19. S. Gao, M. Martcheva, H. Miao, L. Rong, The impact of vaccination on human papillomavirus infection with disassortative geographical mixing: A two-patch modeling study, *J. Math. Biol.*, **84** (2022), 43. https://doi.org/10.1007/s00285-022-01745-z

20. S. Gao, M. Martcheva, H. Miao, L. Rong, A two-sex model of human papillomavirus infection: Vaccination strategies and a case study, *J. Theoret. Biol.*, **536** (2022), 111006. https://doi.org/10.1016/j.jtbi.2022.111006
21. F. Saldaña, J. A. Camacho-Gutiérrez, G. Villavicencio-Pulido, J. X. Velasco-Hernandez, Modeling the transmission dynamics and vaccination strategies for human papillomavirus infection: An optimal control approach, *Appl. Math. Modell.*, **112** (2022), 767–785. https://doi.org/10.1016/j.apm.2022.08.017
22. M. Al-arydah, R. Smith, An age-structured model of human papillomavirus vaccination, *Math. Comput. Simul.*, **82** (2011), 629–652. https://doi.org/10.1016/j.matcom.2011.10.006
23. Z. Afzal, M. Alshehri, Fractional-order SIR model for ADHD as a neurobiological and genetic disorder, *Sci. Rep.*, **15** (2025), 22992. https://doi.org/10.1038/s41598-025-07646-7
24. B. C. Agbata, R. Dervishi, D. F. Agbebaku, E. Cenaj, O. C. Collins, A. U. Ezeafulukwe, et al., A comprehensive analysis of fractional-order model of tuberculosis with treatment intervention, *BMC Infect. Dis.*, **25** (2025), 1070. https://doi.org/10.1186/s12879-025-11303-9
25. Y. Chen, F. Liu, Q. Yu, T. Li, Review of fractional epidemic models, *Appl. Math. Modell.*, **97** (2021), 281–307. https://doi.org/10.1016/j.apm.2021.03.044
26. Z. U. A. Zafar, M. T. Hussain, M. Inc, D. Baleanu, B. Almohsen, A. S. Oke, et al., Fractional-order dynamics of human papillomavirus, *Results Phys.*, **34** (2022), 105281. https://doi.org/10.1016/j.rinp.2022.105281
27. U. K. Nwajeri, A. Omame, C. P. Onyenegecha, Analysis of a fractional order model for HPV and CT co-infection, *Results Phys.*, **28** (2021), 104643. https://doi.org/10.1016/j.rinp.2021.104643
28. A. El-Mesady, T. M. Al-shami, H. M. Ali, Optimal control efforts to reduce the transmission of HPV in a fractional-order mathematical model, *Bound. Value Probl.*, **2025** (2025), 1–39. https://doi.org/10.1186/s13661-024-01991-8
29. M. C. Bahi, S. Bahramand, R. Jan, S. Boulaaras, H. Ahmad, R. Guefaifia, Fractional view analysis of sexual transmitted human papilloma virus infection for public health, *Sci. Rep.*, **14** (2024), 3048. https://doi.org/10.1038/s41598-024-53696-8
30. B. Bajjah, M. Modanli, Finite difference method for infection model of HPV with cervical cancer under Caputo operator, *Discrete Dyn. Nat. Soc.*, **2024** (2024), 2580745. https://doi.org/10.1155/2024/2580745
31. N. Raza, A. Raza, Y. Chahlaoui, J. Gomez-Aguilar, Numerical analysis of hpv HPV and its association with cervical cancer using Atangana–Baleanu fractional derivative, *Modell. Earth Syst. Environ.*, **11** (2025), 60. https://doi.org/10.1007/s40808-024-02243-5
32. P. K. Rajan, M. Kuppusamy, A. Yusuf, A fractional-order modeling of human papillomavirus transmission and cervical cancer, *Model. Earth Syst. Environ.*, **10** (2024), 1337–1357. https://doi.org/10.1007/s40808-023-01843-x
33. P. K. Rajan, M. Kuppusamy, A fractional order human papillomavirus model with Caputo derivative, *J. Anal.*, **32** (2024), 2135–2156. https://doi.org/10.1007/s41478-023-00641-z
34. K. Hattaf, A new mixed fractional derivative with applications in computational biology, *Computation*, **12** (2024), 7. https://doi.org/10.3390/computation12010007

35. K. Hattaf, Useful results for the qualitative analysis of generalized Hattaf mixed fractional differential equations with applications to medicine, *Computation*, **13** (2025), 167. https://doi.org/10.3390/computation13070167
36. F. Assadiki, K. Hattaf, N. Yousfi, Global stability of fractional partial differential equations applied to the biological system modeling a viral infection with Hattaf time-fractional derivative, *Math. Model. Comput.*, **11** (2024), 430–437. https://doi.org/10.23939/mmc2024.02.430
37. S. Bhatter, S. Kumawat, S. D. Purohit, D. Suthar, Mathematical modeling of tuberculosis using Caputo fractional derivative: A comparative analysis with real data, *Sci. Rep.*, **15** (2025), 12672. https://doi.org/10.1038/s41598-025-97502-5
38. E. Kharazmi, M. Cai, X. Zheng, Z. Zhang, G. Lin, G. E. Karniadakis, Identifiability and predictability of integer and fractional-order epidemiological models using physics-informed neural networks, *Nat. Comput. Sci.*, **1** (2021), 744–753. https://doi.org/10.1038/s43588-021-00158-0
39. A. Morán-Torres, N. G. Pazos-Salazar, S. Téllez-Lorenzo, R. Jiménez-Lima, M. Lizano, D. O. Reyes-Hernández, et al., HPV oral and oropharynx infection dynamics in young population, *Braz. J. Microbiol.*, **52** (2021), 1991–2000. https://doi.org/10.1007/s42770-021-00602-3
40. S. L. Ranjeva, E. B. Baskerville, V. Dukic, L. L. Villa, E. Lazcano-Ponce, A. R. Giuliano, et al., Recurring infection with ecologically distinct HPV types can explain high prevalence and diversity, *Proc. Natl. Acad. Sci. U.S.A.*, **114** (2017), 13573–13578. https://doi.org/10.1073/pnas.1714712114
41. H. Trottier, S. Ferreira, P. Thomann, M. C. Costa, J. S. Sobrinho, J. C. M. Prado, et al., Human papillomavirus infection and reinfection in adult women: The role of sexual activity and natural immunity, *Cancer. Res.*, **70** (2010), 8569–8577. https://doi.org/10.1158/0008-5472.CAN-10-0621
42. *Wikipedia Contributors. Caputo Fractional Derivative—Wikipedia, The Free Encyclopedia*. Avaiable from:https://en.wikipedia.org/w/index.php?title=Caputo_fractional_derivative&oldid=1274649699.
43. H. Jahanshahi, J. M. Munoz-Pacheco, S. Bekiros, N. D. Alotaibi, A fractional-order SIRD model with time-dependent memory indexes for encompassing the multi-fractional characteristics of the COVID-19, *Chaos Solitons Fractals*, **143** (2021), 110632. https://doi.org/10.1016/j.chaos.2020.110632
44. J. M. Munoz-Pacheco, C. Posadas-Castillo, E. Zambrano-Serrano, The effect of a non-local fractional operator in an asymmetrical glucose-insulin regulatory system: Analysis, synchronization and electronic implementation, *Symmetry*, **12** (2020), 1395. https://doi.org/10.3390/sym12091395
45. J. Gómez-Aguilar, J. Rosales-García, J. Bernal-Alvarado, T. Córdova-Fraga, R. Guzmán-Cabrera, Fractional mechanical oscillators, *Rev. Mex. Fis.*, **58** (2012), 348–352.
46. P. Van den Driessche, J. Watmough, Reproduction numbers and sub-threshold endemic equilibria for compartmental models of disease transmission, *Math. Biosci.*, **180** (2002), 29–48. https://doi.org/10.1016/S0025-5564(02)00108-6
47. D. Matignon, Stability results for fractional differential equations with applications to control processing, *Comput. Eng. Syst. Appl.*, **2** (1996), 963–968.

48. Z. M. Odibat, Analytic study on linear systems of fractional differential equations, *Comput. Math. Appl.*, **59** (2010), 1171–1183. https://doi.org/10.1016/j.camwa.2009.06.035

49. C. Vargas-De-León, Volterra-type Lyapunov functions for fractional-order epidemic systems, *Commun. Nonlinear Sci. Numer. Simul.*, **24** (2015), 75–85. https://doi.org/10.1016/j.cnsns.2014.12.013

50. J. LaSalle, Limiting equations and stability of nonautonomous ordinary differential equations, in *The Stability of Dynamical Systems*, Society for Industrial and Applied Mathematics, (1976), 57–76.

51. J. A. Gallegos, M. A. Duarte-Mermoud, On the Lyapunov theory for fractional order systems, *Appl. Math. Comput.*, **287** (2016), 161–170. https://doi.org/10.1016/j.amc.2016.04.039

52. K. K. Ang, J. Harris, R. Wheeler, R. Weber, D. I. Rosenthal, P. F. Nguyen-Tân, et al., Human papillomavirus and survival of patients with oropharyngeal cancer, *N. Engl. J. Med.*, **363** (2010), 24–35. https://doi.org/10.1056/NEJMoa0912217

53. A. K. Chaturvedi, E. A. Engels, R. M. Pfeiffer, B. Y. Hernandez, W. Xiao, E. Kim, et al., Human papillomavirus and rising oropharyngeal cancer incidence in the United States, *J. Clin. Oncol.*, **29** (2011), 4294–4301. https://doi.org/0.1200/JCO.2011.36.4596

54. S. R. Khode, R. C. Dwivedi, P. Rhys-Evans, R. Kazi, Exploring the link between human papilloma virus and oral and oropharyngeal cancers, *J. Cancer. Res. Ther.*, **10** (2014), 492–498. https://doi.org/10.4103/0973-1482.138213

55. E. Kokkinis, N. S. Bastas, I. Mega, C. Tsironis, A. D. Lianou, Association of HPV with oral and oropharyngeal cancer: Current evidence, *Maedica*, **19** (2024), 801–806.

56. M. Lechner, J. Liu, L. Masterson, T. R. Fenton, HPV-associated oropharyngeal cancer: Epidemiology, molecular biology and clinical management, *Nat. Rev. Clin. Oncol.*, **19** (2022), 306–327. https://doi.org/10.1038/s41571-022-00603-7

57. H. Damgacioglu, K. Sonawane, Y. Zhu, R. Li, B. A. Balasubramanian, D. R. Lairson, et al., Oropharyngeal cancer incidence and mortality trends in all 50 states in the US, 2001–2017, *JAMA Otolaryngol. Head Neck Surg.*, **148** (2022), 155–165. https://doi.org/10.1001/jamaoto.2021.3567

58. M. Ervik, F. Lam, M. Laversanne, M. Colombet, J. Ferlay, A. Miranda-Filho, et al., *Global Cancer Observatory: Cancer Over Time. Lyon, France: International Agency for Research on Cancer*. Avaiable from:https://gco.iarc.fr/overtime.

59. O. Chiş, J. R. Banga, E. Balsa-Canto, GenSSI: A software toolbox for structural identifiability analysis of biological models, *Bioinformatics*, **27** (2011), 2610–2611. https://doi.org/10.1093/bioinformatics/btr431

60. H. Hong, A. Ovchinnikov, G. Pogudin, C. Yap, SIAN: Software for structural identifiability analysis of ODE models, *Bioinformatics*, **35** (2019), 2873–2874. https://doi.org/10.1093/bioinformatics/bty1069

61. G. Bellu, M. P. Saccomani, S. Audoly, L. D'Angiò, DAISY: A new software tool to test global identifiability of biological and physiological systems, *Comput. Methods Programs Biomed.*, **88** (2007), 52–61. https://doi.org/10.1016/j.cmpb.2007.07.002

62. M. Gultekin, S. Dundar, B. Keskinkilic, M. Turkyilmaz, N. Ozgul, K. Yuce, et al., How to triage HPV positive cases: Results of four million females, *Gynecol. Oncol.*, **158** (2020), 105–111. https://doi.org/10.1016/j.ygyno.2020.04.698

63. H. Miao, X. Xia, A. S. Perelson, H. Wu, On identifiability of nonlinear ODE models and applications in viral dynamics, *SIAM Rev.*, **53** (2011), 3–39. https://doi.org/10.1137/090757009

64. O. R. Isik, N. Tuncer, M. Marctheva, Mathematical model of measles in Turkey, *J. Biol. Syst.*, **32** (2024), 941–970. https://doi.org/10.1142/S0218339024500323

65. N. Tuncer, M. Marctheva, B. LaBarre, S. Payoute, Structural and practical identifiability analysis of zika epidemiological models, *Bull. Math. Biol.*, **80** (2018), 2209–2241. https://doi.org/10.1007/s11538-018-0453-z

66. K. Diethelm, A. D. Freed, The fracPECE subroutine for the numerical solution of differential equations of fractional order, in *Orschung und Wissenschaftliches Rechnen: Beiträge zum Heinz-Billing-Preis 1998*, (1999), 57–71.

67. R. Garrappa, Numerical solution of fractional differential equations: A survey and a software tutorial. *Mathematics*, **6** (2018), 16. https://doi.org/10.3390/math6020016

68. A. Zinihi, Identifying memory effects in epidemics via a fractional SEIRD model and physics-informed neural networks, preprint, arXiv:2509.22760. https://doi.org/10.48550/arXiv.2509.22760

Appendix

If f has the dimension of a number of people (as our state variables in the systems (2.1)–(2.4)), then when we consider the dimensions of each term of the left-hand side of the systems (2.1)–(2.4) with

$$\gamma^{\alpha-1}\mathbf{D}_t^\alpha f(t) = \frac{\gamma^{\alpha-1}}{\Gamma(\alpha)}\int_0^t \frac{f'(s)}{(t-s)^\alpha}ds$$

the dimensions of f' are $\frac{\text{number of people}}{\text{time}}$, $\Gamma(\alpha)$ is dimensionless, $\frac{1}{(t-s)^\alpha}$ is $\frac{1}{\text{time}^\alpha}$, and ds is time. Then $\int_0^t \frac{f'(s)}{(t-s)^\alpha}ds \rightarrow \frac{\text{number of people}}{\text{time}^{\alpha+1}}\text{time} = \frac{\text{number of people}}{\text{time}^\alpha} = \text{number of people}\left[\frac{1}{\text{time}}\right]^\alpha = \text{number of people(time)}^{-\alpha}$. The right-hand side of the systems (2.1)–(2.4) has the dimension $\frac{number of people}{time}$. To make the dimensions of the right-hand side and left-hand side of (2.1)–(2.4) consistent, we multiply it by $\gamma^{\alpha-1}$ since the dimension of $[\gamma]$ is *time* and $[\gamma^{\alpha-1}]$ is $[time]^{\alpha-1}$, the dimension of the left-hand side $[\gamma^{\alpha-1}\mathbf{D}_t^\alpha f(t)]$ is $(\text{time})^{\alpha-1}\text{number of people(time)}^{-\alpha} = \frac{\text{number of people}}{\text{time}}$. Hence, the dimensions of both sides now match.